PA28γ is involved in the degradation of the steroid receptor coactivator 3 (SRC-3) in an ATP- and ubiquitin-independent manner (27). It is still unclear what E3 ubiquitin ligase is responsible for ubiquitylation of the HCV core protein.

E6AP was initially identified as the cellular factor that stimulates ubiquitin-mediated degradation of the tumor suppressor p53 in conjunction with the E6 protein of cancer-associated human papillomavirus types 16 and 18 (14, 48). The E6-E6AP complex functions as a E3 ubiquitin ligase in the ubiquitylation of p53 (49). E6AP is the prototype of a family of ubiquitin ligases called HECT domain ubiquitin ligases, all of which contain a domain *h*omologous to the *E*6AP *c*arboxyl *t*erminus (13). Interestingly, E6AP is not involved in the regulation of p53 ubiquitylation in the absence of E6 (55). Several potential E6-independent substrates for E6AP have been identified, such as hHR23A, Blk, and Mcm7 (23, 24, 35). E6AP is also a candidate gene for Angelman syndrome, which is a severe neurological disorder characterized by mental retardation (21).

This study aimed to identify endogenous ubiquitin-proteasome pathway proteins that are associated with HCV core protein. Tandem affinity purification and mass spectrometry analysis identified E6AP as an HCV core-binding protein. Here we present evidence that E6AP associates with HCV core protein in vitro and in vivo and is involved in ubiquitylation and degradation of HCV core protein. We propose that an E6AP-mediated ubiquitin-proteasome pathway may affect the production of HCV particles through controlling the amounts of HCV core protein.

MATERIALS AND METHODS

Cell culture and transfection. Human embryonic kidney 293T cells, human hepatoblastoma HepG2 cells, and human hepatoma Huh-7 cells were cultured in Dulbecco's modified Eagle's medium (Sigma) supplemented with 50 IU/ml penicillin, 50 μg/ml streptomycin (Invitrogen), and 10% (vol/vol) fetal bovine serum (JRH Biosciences) at 37°C in a 5% CO_2 incubator. 293T cells and HepG2 cells were transfected with plasmid DNA using FuGene 6 transfection reagents (Roche). Huh-7 cells were transfected with plasmid DNA using *Trans*IT LT1 transfection reagents (Mirus).

Plasmids and recombinant baculoviruses. MEF tag cassette (containing *m*yc tag, the tobacco etch virus protease cleavage site, and *F*LAG tag) (16) was fused to the N terminus of the cDNA encoding core protein of HCV NIHJ1 (genotype 1b) (1). To express MEF-tagged core protein in mammalian cells, the genome coding for HCV core protein (amino acids 1 to 191) was amplified by PCR using pBR HCV NIHJ1 as a template. Sense oligonucleotide containing a Kozak consensus translation initiation codon and antisense oligonucleotide containing an in-frame translation stop codon were synthesized by PCR. The amplified PCR product was purified, digested with EcoRI and EcoRV, and then inserted into the EcoRI-EcoRV site of pcDNA3-MEF. FLAG-tagged HCV core expression plasmids based upon pCAGGS (34) were described previously (30). To express E6AP and the active-site cysteine-to-alanine mutant of E6AP in mammalian cells, pCMV4-HA-E6AP isoform II and pCMV4-HA-E6AP C-A were utilized (19). The C-A mutation was introduced at the site of E6AP C843. To express E6AP and E6AP C-A under the CAG promoter, the E6AP fragment and the E6AP C-A fragment were amplified by PCR, purified, digested with SmaI and NotI, and blunt ended using a DNA blunting kit (Takara). These PCR fragments were subcloned into pCAGGS.

To make a fusion protein consisting of glutathione *S*-transferase (GST) fused to the N terminus of E6AP in *Escherichia coli*, the E6AP fragment was amplified by PCR and the resultant product was cloned into the SmaI-NotI site of pGEX4T-1 vector (Amersham Biosciences). To express a series of E6AP truncation mutants as GST fusion proteins, each fragment was amplified by PCR and cloned into the SmaI-NotI site of pGEX4T-1. To purify GST core protein efficiently by two-step affinity purification, we fused hexahistidine (His) tag to the C terminus of GST fusion proteins. To bacterially express HCV core (aa 1 to 173) protein as a fusion protein containing N-terminal GST tag and C-terminal His tag, core fragment was amplified by PCR and the resultant product was cloned into the EcoRI-NotI site of pGEX4T-1 vector. The resultant plasmid was designated pGEX GST-C173HT. To express GST core (1–152)-His and GST-His in *E. coli*, pGEX core (1–152)-His and pGEX-His were constructed similarly. The resultant plasmids were designated pGEX GST-C152HT and pGEX GST-HT, respectively.

To generate recombinant baculoviruses expressing GST-E6AP, GST-E6AP fragment was excised from pGEX E6AP by digestion with SmaI and Tth111I and ligated into the SmaI-Tth111I site of pVL1392 (Invitrogen). To express GST-E6AP C-A, pVLGST-E6AP C-A was constructed similarly. To generate recombinant baculovirus expressing HCV core (aa 1 to 173) protein as a fusion protein containing N-terminal GST tag and C-terminal His tag, GST-C173HT fragment was amplified by PCR using pGEX GST-C173HT as a template, digested with BglII-XbaI, and subcloned into the BglII-XbaI site of pVL1392. To generate recombinant baculoviruses expressing GST-C152HT and GST-HT, cDNA fragments corresponding to GST-C152HT and GST-HT were amplified by PCR and subcloned into pVL1392, respectively. The resultant plasmids were designated pVLGST-C173HT, pVLGST-C152HT, and pVLGST-HT. To generate recombinant baculovirus expressing MEF-tagged E6AP, cDNA fragment encoding MEF-E6AP was subcloned into pVL1392. To express HCV core protein in the TNT-coupled wheat germ lysate system (Promega), HCV core cDNA was inserted in the EcoRI site of pCMV1NT (Promega). The primer sequences used in this study are available from the authors upon request. The sequences of the inserts were extensively verified using an ABI PRISM 3100-Avant Genetic Analyzer (Applied Biosystems). Recombinant baculoviruses were recovered using a BaculoGold transfection kit (Pharmingen) according to the manufacturer's instructions.

Antibodies. The mouse monoclonal antibodies (MAbs) used in this study were anti-hemagglutinin (anti-HA) MAb (12CA5; Roche), anti-FLAG (M2) MAb (Sigma), anti-c-*myc* MAb (9E10; Santa Cruz), anti-glyceraldehyde-3-phosphate dehydrogenase (anti-GAPDH) MAb (Chemicon), anti-GST MAb (Santa Cruz), anti-ubiquitin MAb (Chemicon), anti-E6AP MAb (E6AP-330) (Sigma), anticore MAb (B2; Anogen), and another anti-core MAb (2H9) (56). Polyclonal antibodies (PAbs) used in this study were anti-HA rabbit PAb (Y-11; Santa Cruz), anti-FLAG rabbit PAb (F7425; Sigma), anti-E6AP rabbit PAb (H-182; Santa Cruz), anti-DDX3 rabbit PAb (47), anti-PA28γ rabbit PAb (Affiniti), and anti-GST goat PAb (Amersham). Anticore rabbit PAb (TS1) was raised against the recombinant GST core protein.

MEF purification procedure. 293T cells were transfected with the plasmid expressing MEF core by the calcium phosphate precipitation method (4). After the cells were lysed, the expressed MEF core and its binding proteins were recovered following the procedure described previously (16). 293T cells transfected with pcDNA3-MEF core in four 10-cm dishes were lysed in 2 ml of lysis buffer: 50 mM Tris-HCl (pH 7.5), 150 mM NaCl, 10% (wt/vol) glycerol, 100 mM NaF, 1 mM Na_3VO_4, 1% (wt/vol) Triton X-100, 5 μM $ZnCl_2$, 2 mM phenylmethylsulfonyl fluoride, 10 μg/ml aprotinin, and 1 μg/ml leupeptin. The lysate was centrifuged at 100,000 × *g* for 20 min at 4°C. The supernatant was passed through a 5-μm filter, incubated with 100 μl of Sepharose beads for 60 min at 4°C, and then passed through a 0.65-μm filter. The filtered supernatant was mixed with 100 μl of anti-myc-conjugated Sepharose beads for the first immunoprecipitation. After incubation for 90 min at 4°C, the beads were washed five times with 1 ml of TNTG buffer (20 mM Tris-HCl, pH 7.5, 150 mM NaCl, 10% [wt/vol] glycerol, and 1% [wt/vol] Triton X-100), twice with 1 ml of buffer A (20 mM Tris-HCl, pH 7.5, 150 mM NaCl, and 1% [wt/vol] Triton X-100), and finally once with 1 ml of TNT buffer (50 mM Tris-HCl, pH 8.0, 150 mM NaCl, 1% [wt/vol] Triton X-100). The washed beads were incubated with 10 U of tobacco etch virus protease (Invitrogen) in TNT buffer (100 μl) to release bound protein complexes from the beads. After incubation for 60 min at room temperature, the supernatant was pooled and the beads were washed twice with 70 μl of buffer A. The resulting supernatants were combined and incubated with 12 μl of FLAG-Sepharose beads for the second immunoprecipitation. After incubation for 60 min at room temperature, the beads were washed three times with 240 μl of buffer A, and proteins bound to the immobilized HCV core protein on the FLAG beads were dissociated by incubation with 80 μg/ml FLAG peptide (NH_2-Asp-Tyr-Lys-Asp-Asp-Asp-Asp-Lys-COOH) (Sigma).

MS/MS. Proteins were separated by 9% sodium dodecyl sulfate-polyacrylamide gel electrophoresis (SDS-PAGE) and visualized by silver staining. The stained bands were excised and digested in the gel with lysylendoprotease-C (Lys-C), and the resulting peptide mixtures were analyzed using a direct nanoflow liquid chromatography-tandem mass spectrometry (MS/MS) system (33), equipped with an electrospray interface reversed-phase column, a nanoflow gradient device, a high-resolution Q-time of flight hybrid mass spectrometer (Q-TOF2; Micromass), and an automated data analysis system. All the MS/MS

spectra were searched against the nonredundant protein sequence database maintained at the National Center for Biotechnology Information using the Mascot program (Matrixscience) to identify proteins. The MS/MS signal assignments were also confirmed manually.

Expression and purification of recombinant proteins. *E. coli* BL21(DE3) cells were transformed with plasmids expressing GST fusion protein or His-tagged protein and grown at 37°C. Expression of the fusion protein was induced by 1 mM isopropyl-β-D-thiogalactopyranoside at 37°C for 4 h. Bacteria were harvested, suspended in lysis buffer (phosphate-buffered saline [PBS] containing 1% Triton X-100), and sonicated on ice.

Hi5 cells were infected with recombinant baculoviruses to produce GST-C173HT, GST-C152HT, GST-HT, MEF-E6AP, and His-tagged mouse E1 (17). GST and GST fusion proteins were purified on glutathione-Sepharose beads (Amersham Bioscience) according to the manufacturer's protocols. His-tagged proteins were purified on nickel-nitrilotriacetic acid beads (QIAGEN) according to the manufacturer's protocols. MEF-E6AP and MEF-E6AP C-A were purified on anti-FLAG M2 agarose beads (Sigma) according to the manufacturer's protocols.

Immunoblot analysis. Immunoblot analysis was performed essentially as described previously (11). The membrane was visualized with SuperSignal West Pico chemiluminescent substrate (Pierce).

HCV core protein and E6AP binding assays. To map the E6AP binding site on HCV core protein, 2.5 μg of purified recombinant GST-E6AP expressed in Hi5 cells was mixed with 1,000 μg of 293T cell lysates transfected with a series of FLAG-tagged HCV core deletion mutants as indicated. The protein concentration of the cells was determined using the bicinchoninic acid protein assay kit (Pierce). The mixtures were immunoprecipitated with anti-FLAG M2 agarose beads (Sigma), and proteins bound to the immobilized HCV core protein on anti-FLAG beads were dissociated with FLAG peptide (Sigma). The eluates were analyzed by immunoblotting with anti-GST PAb. To map the HCV core-binding site on E6AP, GST pull-down assays were performed as described previously (51).

In vivo ubiquitylation assay. In vivo ubiquitylation assays were performed essentially as described previously (57). FLAG-core was immunoprecipitated with anti-FLAG beads. Immunoprecipitates were analyzed by immunoblotting, using either anti-HA PAb or anticore PAb (TS1) to detect ubiquitylated core proteins.

In vitro ubiquitylation assay. For in vitro ubiquitylation of HCV core protein, purified GST-C173HT and GST-C152HT were used as substrates. Purified GST-HT was used as a negative control. Assays were done in 40-μl volumes containing 20 mM Tris-HCl, pH 7.6, 50 mM NaCl, 5 mM ATP, 10 mM $MgCl_2$, 8 μg of bovine ubiquitin (Sigma), 0.1 mM dithiothreitol, 200 ng mouse E1, 200 ng E2 (UbcH7), and 0.5 μg each of MEF-E6AP or MEF-E6AP C-A. The reaction mixtures were incubated at 37°C for 120 min followed by purification with glutathione-Sepharose beads and immunoblotting with the indicated antibodies.

siRNA transfection. 293T cells or Huh-7 cells at 3×10^5 cells in a six-well plate were transfected with 40 pmol of either E6AP-specific short interfering RNA (siRNA; Sigma) or scramble negative-control siRNA duplexes (Sigma) using HiPerFect transfection reagent (QIAGEN) following the manufacturer's instructions. The siRNA target sequences were as follows: E6AP (sense), 5′-GGGUC UACACCAGAUUGCUTT-3′; scramble negative control (sense), 5′-UUGCG GGUCUAAUCACCGATT-3′.

CHX half-life experiments. To examine the half-life of HCV core protein, transfected 293T cells were treated with 50 μg/ml cycloheximide (CHX) at 44 h posttransfection. The cells at zero time points were harvested immediately after treatment with CHX. Cells from subsequent time points were incubated in medium containing CHX at 37°C for 3, 6, and 9 h as indicated.

Infection of Huh-7 cells with secreted HCV. Infectious HCV JFH1 was produced in Huh-7.5.1 cells (61) as described previously (56). Culture supernatant containing infectious HCV JFH1 was collected and passed through a 0.22-μm filter. Naive Huh-7 cells were seeded 24 h before infection at a density of 1×10^6 in a 10-cm dish. The cells were incubated with 2.5 ml of the inoculum (6.5×10^3 50% tissue culture infectious dose [$TCID_{50}$]/ml) for 3 h, washed three times with PBS, and supplemented with fresh complete Dulbecco's modified Eagle's medium. Then the cells were transfected with 6 μg each of pCAGGS, pCAG-HA-E6AP, or pCAG-HA-E6AP C-A by using TransIT LT1 (Mirus). The cells were trypsinized and replated in six-well plates at 1 day postinfection. The culture medium was changed every 2 days. The culture supernatants and the cells were collected at days 3 and 7 postinfection.

Quantitation of HCV RNA and core protein. We quantitated HCV core protein in cell lysate using the HCV core antigen enzyme-linked immunosorbent assay (ELISA) (Ortho-Clinical Diagnostics). Total RNA was extracted from cells using TRIzol reagent (Invitrogen). To quantitate HCV RNAs, real-time reverse transcription-PCR was performed as described previously (53).

Infectivity assay. The $TCID_{50}$ was calculated essentially based on the method described previously (28). Virus titration was performed by seeding Huh-7 cells in 96-well plates at 1×10^4 cells/well. Samples were serially diluted fivefold in complete growth medium and used to infect the seeded cells (six wells per dilution). Following 3 days of incubation, the cells were immunostained for core with anticore MAb (2H9). Wells that expressed at least one core-expressing cell were counted as positive, and the $TCID_{50}$ was calculated.

Immunocytochemistry and fluorescence microscopy. Cells on collagen-coated coverslips were washed with PBS, fixed with 4% paraformaldehyde for 30 min at 4°C, and permeabilized with PBS containing 0.2% Triton X-100. Cells were preincubated with BlockAce (Dainippon Pharmaceuticals), incubated with specific antibodies as primary antibodies, washed, and incubated with rhodamine-conjugated goat anti-rabbit immunoglobulin G (ICN Pharmaceuticals, Inc.) and Qdot 565-conjugated goat anti-mouse immunoglobulin G (Quantumdot) as secondary antibody. Then the cells were washed with PBS, counterstained with DAPI (4′,6′-diamidino-2-phenylindole) solution (Sigma) for 3 min, mounted on glass slides, and examined with a BZ-8000 microscope (Keyence).

Knockdown of endogenous E6AP in HCV JFH1-infected Huh-7 cells. Naive Huh-7 cells at 10^6 cells/10-cm dish were inoculated with 2.5 ml of the inoculum including infectious HCV JFH1 (6.5×10^3 $TCID_{50}$/ml) and cultured. The cells were replated in a six-well plate at 3×10^5 cells/well at day 11 postinfection and transfected with 40 pmol of E6AP siRNA or control siRNA. The culture medium was changed at 24 h after transfection. The cells were harvested at day 2 after transfection, and the intracellular core protein levels were quantitated using the HCV core antigen ELISA. The culture supernatants were collected at day 2 after transfection and assayed for $TCID_{50}$ determinations.

RESULTS

Identification of E6AP as an HCV core-binding protein. To identify the molecular machinery for HCV core ubiquitylation, we searched for endogenous ubiquitin-proteasome pathway proteins that associated with HCV core protein. HCV core-binding proteins (i.e., MEF core and its binding proteins, recovered from lysed cells) were purified by a tandem affinity purification procedure using a tandem tag (known as MEF tag) (16). Ten proteins were reproducibly detected (Fig. 1A, lane 2), but none were recovered from lysed control cells transfected with empty vector alone (Fig. 1A, lane 1).

To identify the proteins, silver-stained bands were excised from the gel, digested by Lys-C, and analyzed using a direct nanoflow liquid chromatography-MS/MS system. Nine proteins were identified: two known HCV core-binding proteins, human DEAD box protein DDX3 (38) and proteasome activator PA28γ (30), and seven potential HCV core-binding proteins. E6AP was identified (Fig. 1A, lane 2) on the basis of five independent MS/MS spectra (Table 1). Immunoblot analyses confirmed the proteomic identification of E6AP, DDX3, PA28γ, and MEF-core (Fig. 1B to E).

E6AP binding domain for HCV core protein. The E6AP binding domain for HCV core protein was investigated. Figure 2A is a schematic representation of E6AP and known motifs in E6AP. A series of deletion mutants of E6AP as GST fusion proteins were expressed in *E. coli*. GST pull-down assays found that the carboxyl-terminal deletion mutant E6AP (1–517), but not E6AP (1–418) (Fig. 2C, lanes C and D), and the amino-terminal deletion mutant E6AP (418–875), but not E6AP (517–875) (Fig. 2C, lanes J and K), were able to bind to the core protein. The signal was absent when unprogrammed wheat germ extracts (the negative control) were used as a source of proteins (data not shown). GST pull-down assays (Fig. 2B) found that the region from aa 418 to aa 517 is important for binding to the HCV core protein. An assay of the

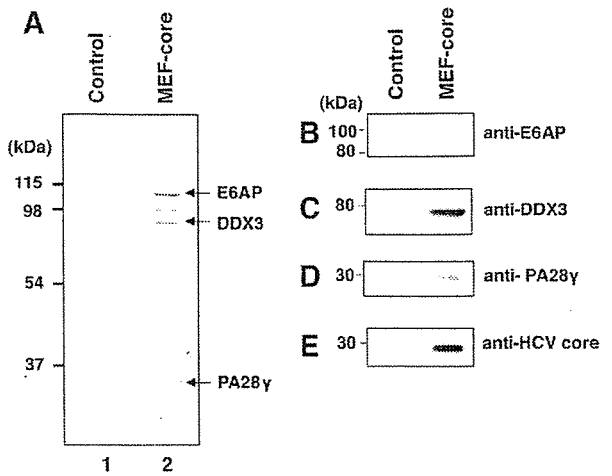

FIG. 1. HCV core protein associates with E6AP in vivo. (A) 293T cells were transfected with pcDNA3-MEF-core or empty plasmid, incubated for 48 h, and then harvested. The expressed MEF-core and binding proteins were recovered using the MEF purification procedure. Proteins bound to the MEF-core immobilized on anti-FLAG beads were dissociated with FLAG peptides, resolved by 9% SDS-PAGE, and visualized by silver staining. Control experiments were performed using 293T cells transfected with vector alone. The positions of E6AP, DDX3, and PA28γ are indicated by arrows. (B to E) The proteins detected in panel A were confirmed by immunoblotting with appropriate antibodies: E6AP (B), DDX3 (C), PA28γ (D), and MEF-core (E).

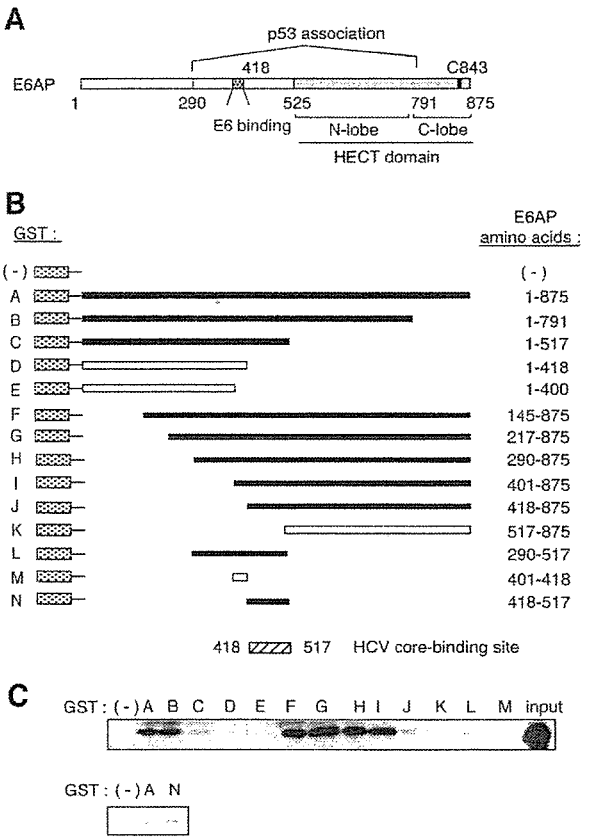

FIG. 2. Mapping of the HCV core-binding domain for E6AP. (A) Structure of E6AP. Shown is a schematic representation of the regions of E6AP isoform II that mediate E6 binding (aa 401 to 418), E6-dependent association with p53 (aa 290 to 791), and the HECT catalytic domain (aa 525 to 875). The catalytic cysteine residue is located at aa 843. (B) Schematic representation of GST-E6AP proteins. GST proteins A through N contain the E6AP amino acids indicated to the right. The shaded region of each represents the GST sequence. Closed boxes represent proteins that are bound specifically to HCV core protein, and open boxes represent those that are not bound. (C) Binding of HCV core protein to GST-E6AP proteins A through N. In vitro-translated core protein (aa 1 to 173) was assayed for association with GST (-) or the GST-E6AP fusion proteins A through N. Association of core protein was detected by immunoblotting with anti-core MAb.

ability of GST-E6AP (418–517) to bind to the HCV core protein was confirmatory (Fig. 2C, lane N) and led to the conclusion that the HCV core-binding domain of E6AP was aa 418 to aa 517.

The HCV core-binding domain for E6AP. By use of a panel of HCV core deletion mutants (Fig. 3A), GST-E6AP was found to coimmunoprecipitate with all of the FLAG-core proteins (Fig. 3A, lanes A to H) except FLAG-core (72–191) or FLAG-core (92–191) (Fig. 3A, lanes I and J). No association of control GST protein with any FLAG-core proteins was observed (data not shown). These data suggest that the aa-58-to-aa-71 segment of the HCV core binds to E6AP. The ability of GST-core (58–71) to associate with purified MEF-E6AP confirmed that the core (aa 58–71) was the site for E6AP binding on the HCV core protein (Fig. 3B).

E6AP decreases steady-state levels of HCV core protein in 293T cells and HepG2 cells. One of the features of HECT domain ubiquitin ligases is direct association with their substrates (50). Thus, we hypothesized that E6AP would function as an E3 ubiquitin ligase for the HCV core protein. We assessed the effects of E6AP on the HCV core protein in 293T cells. FLAG-core (1–191) together with HA-tagged wild-type E6AP, catalytically inactive mutant E6AP, E6AP C-A (19), or WWP1 (another HECT domain ubiquitin ligase) (22) was introduced into 293T cells, and the levels of the core protein were examined by immunoblotting. The steady-state levels of the core protein decreased with an increase in the amount of E6AP plasmids (Fig. 4A and B). However, neither E6AP C-A mutant nor WWP1 decreased the steady-state levels of the core protein, suggesting that E6AP enhances degradation of the core protein.

To verify the critical need for endogenous E6AP in the core degradation, expression of E6AP was knocked down by siRNA and the expression of the core protein and E6AP was assayed by immunoblotting. Transfection of the E6AP-specific siRNA

TABLE 1. Identification of E6AP by tandem mass spectrometry[a]

Peptide *m/z*	Sequence determined	Residues
720.9	VFSSAEALVQSFR	156–168
922.4	AACSAAAMEEDSEASSSR	196–213
774.9	MMETFQQLITYK	339–350
1,053.1	ITVLYSLVQGQQLNPYLR	507–524
809.4	EFVISYSDYILNK	712–724

[a] The protein was ubiquitin protein ligase E3A (E6AP) isoform 2 (GenBank accession no. NP_000453).

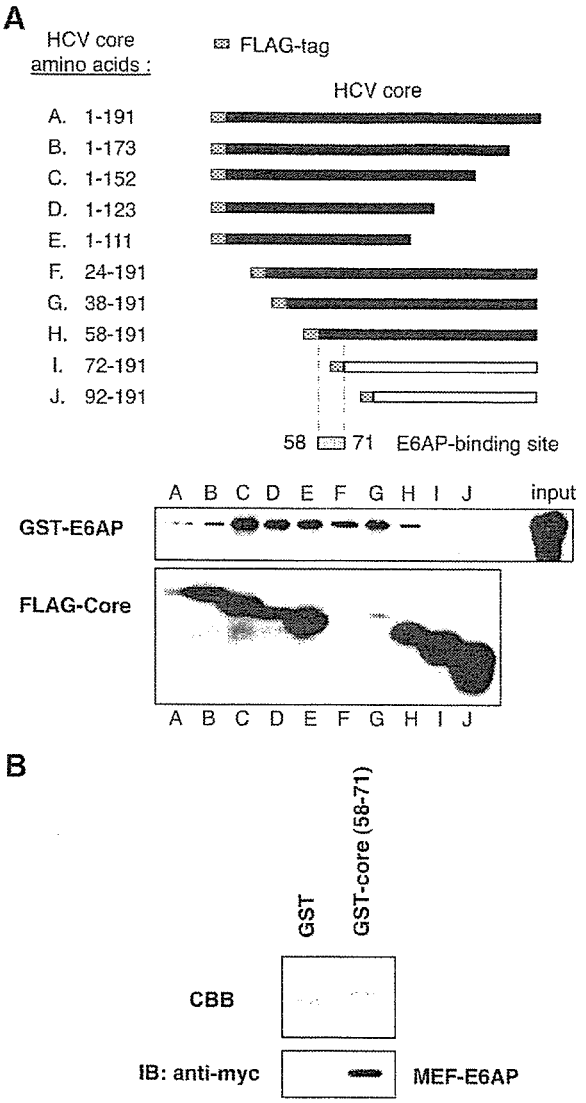

FIG. 3. Mapping of the E6AP binding domain for HCV core protein. (A) In vitro binding of E6AP to HCV core protein. 293T cells were transfected with each plasmid indicated in the upper panel. At 48 h posttransfection, cell lysates were mixed with purified GST-E6AP, immunoprecipitated with anti-FLAG beads, and then immunoblotted with anti-GST PAb (middle panel) or anti-FLAG MAb (bottom panel). The last lane (input) represents GST-E6AP used in this assay (middle panel). (B) Binding of GST-core (aa 58 to aa 71) to purified MEF-E6AP. GST served as a negative control for binding. Upper panel, Coomassie blue-stained SDS-PAGE of GST and GST-core (58–71). Lower panel, results of the GST pull-down assay. MEF-E6AP was detected by anti-myc MAb. CBB, Coomassie brilliant blue; IB, immunoblot.

duplex reduced the protein level of E6AP by 90% at 48 h posttransfection (Fig. 4C, middle panel). Immunoblotting revealed a 4.1-fold increase in the level of the core protein in the cells transfected with E6AP siRNA (Fig. 4C, top panel), suggesting that endogenous E6AP plays a role in the proteolysis of the HCV core protein.

Then we examined whether E6AP reduces the steady-state

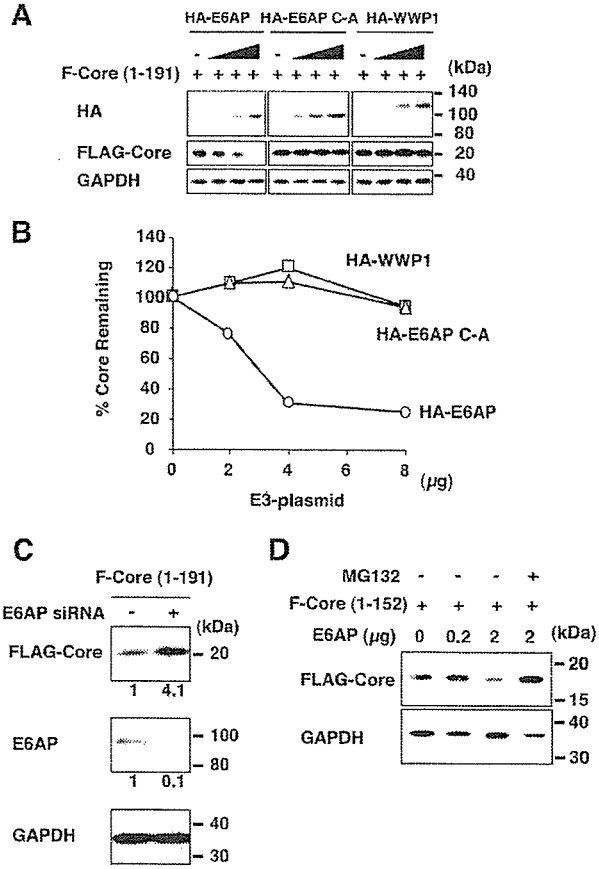

FIG. 4. E6AP decreases steady-state levels of HCV core protein in 293T cells and in HepG2 cells. (A) 293T cells (1×10^6 cells/10-cm dish) were transfected with 1 μg of pCAG FLAG-core (1–191) along with either pCAG-HA-E6AP, pCAG-HA-E6AP C-A, or pCAG-HA-WWP1 as indicated. At 48 h posttransfection, protein extracts were separated by SDS-PAGE and analyzed by immunoblotting with anti-HA PAb (top panel), anti-FLAG MAb (middle panel), and anti-GAPDH MAb (bottom panel). (B) Quantitation of data shown in panel A. Intensities of the gel bands were quantitated using the NIH Image 1.62 program. The level of GAPDH served as a loading control. Circles, E6AP; triangles, E6AP C-A; squares, WWP1. (C) Knockdown of endogenous E6AP by siRNA inhibits degradation of HCV core protein in 293T cells. 293T cells (3×10^5 cells/six-well plate) were transfected with 40 pmol of E6AP-specific duplex siRNA (or control siRNA) as described in Materials and Methods. The cells were transfected with 2 μg of FLAG-core (1–191) expression plasmid and cultured for 24 h, harvested, and analyzed by immunoblotting. Shown is immunoblot detection of FLAG-tagged core protein (top panel), E6AP protein (middle panel), and GAPDH (bottom panel) in control siRNA-treated 293T cells or E6AP-siRNA-treated 293T cells. The relative levels of protein expression were quantitated by densitometry and indicated below in the respective lanes. GAPDH served as a loading control. (D) HepG2 cells (2×10^5 cells/six-well plate) were transfected with pCAG FLAG-core (1–152) along with either empty vector or pCMV E6AP as indicated. The cells were harvested at 44 h posttransfection. Where indicated, cells were treated with 25 μM MG132 or with dimethyl sulfoxide control 14 h prior to collection. Equivalent amounts of the whole-cell lysates were separated by SDS-PAGE and analyzed by immunoblotting with anti-FLAG MAb (upper panel) or anti-GAPDH MAb (lower panel).

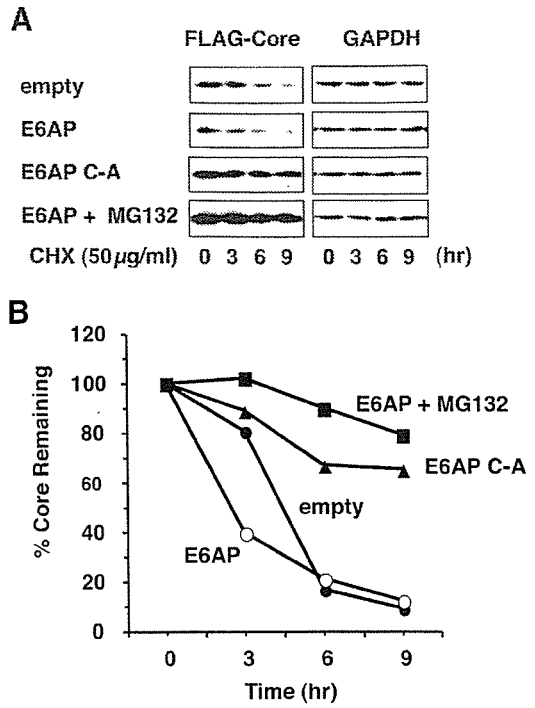

FIG. 5. Kinetic analysis of E6AP-dependent degradation of HCV core protein. (A) 293T cells (1×10^6 cells/10-cm dish) were transfected with 1 μg of pCAG-FLAG core (1–152) plus 4 μg of empty vector, pCMV-HA-E6AP, or pCMV-HA-E6AP C-A. The cells were treated with 50 μg/ml CHX at 44 h after transfection. Cell extracts were collected at 0, 3, 6, and 9 h after treatment with CHX, followed by immunoblotting. (B) Specific signals were quantitated by densitometry, and the percent remaining core at each time was compared with that at the starting point. The level of GAPDH served as a loading control. Open circles, E6AP; closed circles, empty plasmid; closed triangles, E6AP C-A; closed squares, E6AP with MG132 treatment. Data are representative of three independent experimental determinations.

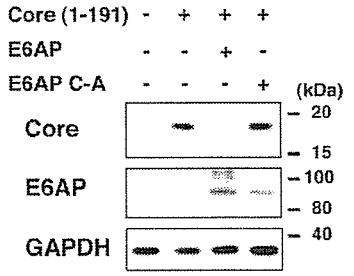

FIG. 6. E6AP promotes degradation of full-length HCV core protein in Huh-7 cells. Huh-7 cells (2×10^5 cells/six-well plate) were transfected with 0.5 μg of pCAG-core (1–191) together with 2 μg of pCMV-HA-E6AP or pCMV-HA-E6AP C-A. At 48 h posttransfection, cells were harvested and analyzed by immunoblotting with anticore MAb (top panel), anti-E6AP PAb (middle panel), or anti-GAPDH MAb (bottom panel).

levels of the core protein in hepatic cells as well as in 293T cells. Exogenous expression of E6AP resulted in reduction of the core protein in human hepatoblastoma HepG2 cells (Fig. 4D). Treatment of the cells with the proteasome inhibitor MG132 increased the core protein level, suggesting that the core protein was degraded through the ubiquitin-proteasome pathway. These results indicate that E6AP enhances proteasomal degradation of the HCV core protein in both hepatic cells and nonhepatic cells.

Kinetic analysis of E6AP-dependent degradation of HCV core protein. To determine whether the E6AP-induced reduction of the core protein is due to an increase in the rate of core degradation, we performed kinetic analysis using the protein synthesis inhibitor CHX. HCV core protein together with wild-type E6AP or inactive mutant E6AP C-A was expressed in 293T cells. At 44 h after transfection, cells were treated with either 50 μg/ml CHX alone or 50 μg/ml CHX plus 25 μM MG132 to inhibit proteasome function. Cells were collected at 0, 3, 6, and 9 h following treatment and analyzed by immunoblotting (Fig. 5A). Overexpression of E6AP resulted in rapid degradation of the core protein, whereas inactive mutant E6AP C-A increased the half-life of the core protein (Fig. 5B), suggesting that the inactive E6AP inhibited degradation of the core protein in a dominant-negative manner, which is in agreement with previous studies (19, 55). Treatment of the cells with MG132 inhibited the degradation of the core protein (Fig. 5B). Reverse transcription-PCR to determine mRNA levels of the HCV core gene and GAPDH gene found that neither wild-type E6AP nor inactive E6AP changed mRNA levels of the HCV core gene and GAPDH gene (data not shown). These results indicate that E6AP enhances proteasomal degradation of the core protein.

E6AP promotes degradation of the full-length core protein in Huh-7 cells. To determine whether the full-length HCV core protein expressed in hepatic cells is degraded through an E6AP-dependent pathway, human hepatoma Huh-7 cells were transfected with pCAG HCV core (1–191) along with either E6AP or E6AP C-A. To rule out the effects of N-terminal FLAG tag on the core degradation, HCV core protein was expressed as untagged protein. Expression of wild-type E6AP resulted in reduction of the core protein (Fig. 6). On the other hand, HCV core protein was not decreased after transfection of inactive E6AP, indicating that the full-length core protein expressed in Huh-7 cells is also degraded through an E6AP-dependent pathway.

E6AP mediates ubiquitylation of HCV core protein in vivo. To determine whether E6AP can induce ubiquitylation of HCV core protein in cells, we performed in vivo ubiquitylation assays. 293T cells were cotransfected with FLAG-core (1–191) and either E6AP or empty plasmid, together with a plasmid encoding HA-tagged ubiquitin to facilitate detection of ubiquitylated core protein. Cell lysates were immunoprecipitated with anti-FLAG MAb and immunoblotted with anti-HA PAb to detect ubiquitylated core protein (Fig. 7A). Only a little ubiquitin signal was observed on the core protein in the absence of cotransfected E6AP (Fig. 7A, lane 3). In contrast, coexpression of E6AP led to readily detectable ubiquitylated forms of the core protein as a ladder and a smear of higher-molecular-weight bands (Fig. 7A, compare lane 3 with lane 4). Immunoblot analysis with anticore PAb confirmed that FLAG-core proteins were immunoprecipitated (Fig. 7B, lanes 2 to 4, short exposure) and that higher-molecular-weight bands con-

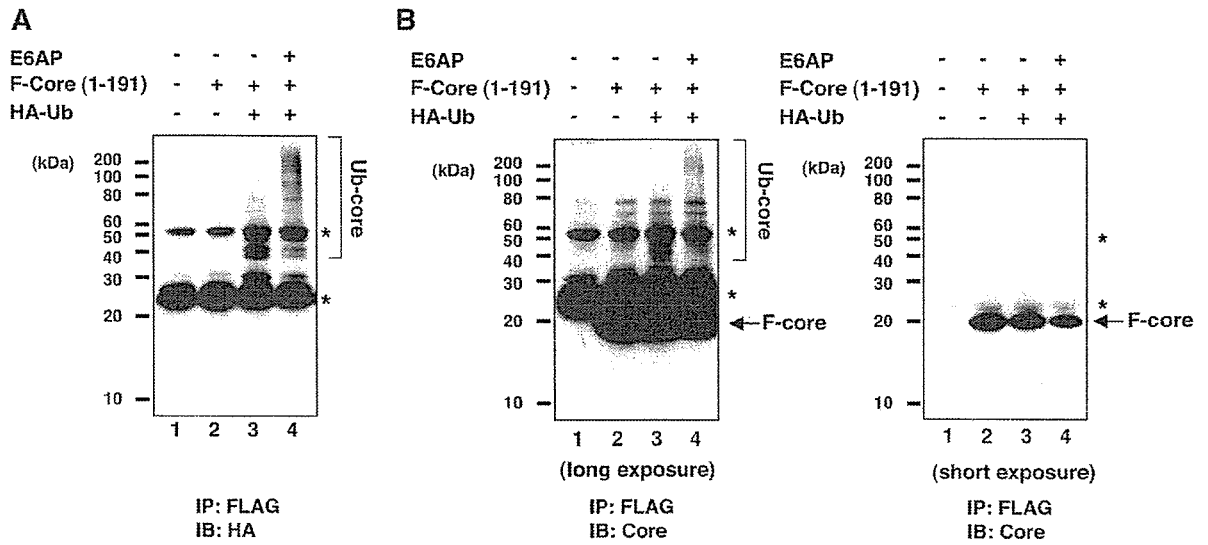

FIG. 7. E6AP-dependent ubiquitylation of HCV core protein in vivo. 293T cells (1×10^6 cells/10-cm dish) were transfected with 1 μg of pCAG FLAG-core (1–191) together with 2 μg of plasmid encoding E6AP as indicated. Each transfection also included 2 μg of plasmid encoding HA-ubiquitin. The cell lysates were immunoprecipitated with FLAG beads and analyzed by immunoblotting with anti-HA PAb (A) or anticore PAb (B). A shorter exposure of the core blot shows immunoprecipitated FLAG-core protein (B, right panel). A longer exposure of the core blot shows the presence of a ubiquitin smear (B, left panel). Asterisks indicate cross-reacting immunoglobulin light chain or heavy chain. Arrows indicate FLAG-core. IB, immunoblot; IP, immunoprecipitation.

jugated with HA-ubiquitin were indeed ubiquitylated forms of the core protein (Fig. 7B, lanes 3 and 4, long exposure).

E6AP mediates ubiquitylation of HCV core protein in vitro. To rule out the possibility that E6AP contributes to core protein degradation by inducing degradation of inhibitors of core turnover, we determined whether E6AP functions directly as a ubiquitin ligase by testing the ability of purified MEF-E6AP to mediate in vitro ubiquitylation of the purified recombinant HCV core protein. HCV core protein was expressed as a fusion protein containing N-terminal GST tag and C-terminal His tag and purified as described in Materials and Methods. GST-C173HT (aa 1–173) and GST-C152HT (aa 1–152) (see Materials and Methods) were used to determine whether the mature core protein and the C-terminally truncated core protein are targeted for ubiquitylation in vitro. The validity of this assay was established by demonstrating that E6AP but not E6AP C-A induced ATP-dependent ubiquitylation of GST-core protein. When in vitro ubiquitylation reactions were carried out either in the absence of MEF-E6AP or in the presence of MEF-E6AP C-A, no ubiquitylation signal was detected (Fig. 8A, lanes 4 and 5). However, inclusion of purified MEF-E6AP in the reaction mixture resulted in marked ubiquitylation of GST-C173HT (Fig. 8A, lane 6), while no ubiquitylation was observed in the absence of ATP (Fig. 8A, lane 7). No signal was detected when GST-HT was used as a substrate (Fig. 8A, lane 8). The higher-molecular-weight species of GST-core proteins were reactive with both anti-ubiquitin MAb (Fig. 8B, right panel, lanes 2 and 4) and anti-GST MAb (Fig. 8B, left panel, lanes 2 and 4). Both GST-C152HT and GST-C173HT were polyubiquitylated by E6AP in vitro (Fig. 8B), indicating that both the C-terminally truncated core and the mature core are polyubiquitylated by E6AP in vitro. These results revealed that E6AP directly mediated ubiquitylation of HCV core proteins in an ATP-dependent manner.

Exogenous expression of E6AP reduces intracellular HCV core protein levels and supernatant infectivity titers in HCV-infected Huh-7 cells. We used a recently developed system for the production of infectious HCV particles using the HCV JFH1 strain (28, 56, 61) to examine whether E6AP can promote degradation of HCV core protein expressed from infectious HCV. E6AP-dependent core degradation was assessed in Huh-7 cells inoculated with the culture supernatant containing HCV JFH1. Levels of HCV core protein were detectable at day 3 postinfection and increased with time. Immunofluorescence staining for the core protein indicated that the percentage of HCV core-positive cells in the Huh-7 cells was almost 100 at day 7 postinfection. Transfection efficiency was 50 to 60% as measured with GFP-expressing plasmid. At day 7 postinfection, exogenous expression of E6AP reduced the intracellular core protein level by about 60% compared to the empty plasmid-transfected control cells (Fig. 9A). Inactive E6AP had little effect on the core protein levels. Total protein levels in the cells (Fig. 9B) and intracellular HCV RNA levels (Fig. 9C) did not change after transfection of wild-type E6AP or inactive E6AP. The immunofluorescence study revealed that HCV core protein was variably detected and the intensity of core staining was reduced in the cells staining positive for wild-type E6AP compared with neighboring cells staining negative for E6AP (Fig. 9E). Using inactive E6AP revealed colocalization of the core protein and E6AP in the perinuclear region (Fig. 9F) of HCV-infected cells. These results suggest that E6AP enhanced degradation of HCV core protein expressed from infectious HCV. Then we titrated HCV infectivity in the culture supernatant at day 7 postinfection by limiting

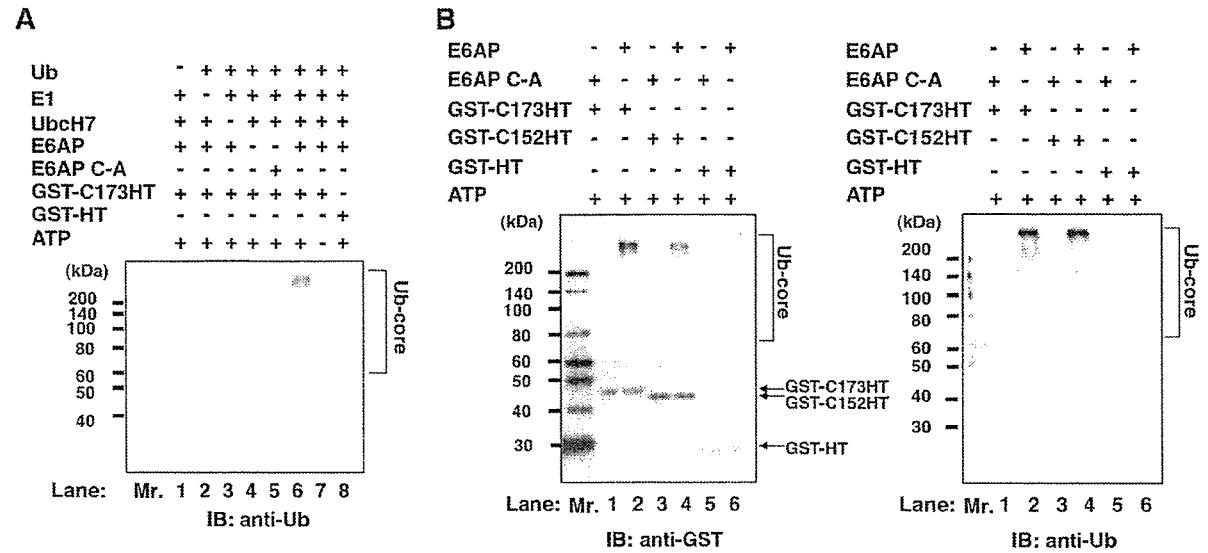

FIG. 8. In vitro ubiquitylation of HCV core protein by recombinant E6AP. For in vitro ubiquitylation of HCV core protein, purified GST-C173HT and GST-C152HT were used as substrates. Purified GST-HT was used as a negative control. Assays were done in 40-μl volumes containing each component as indicated. The reaction mixture is described in Materials and Methods. The reaction was carried out at 37°C for 120 min followed by purification with glutathione-Sepharose beads and analysis by immunoblotting with the indicated antibodies. Arrows indicate GST-C173HT, GST-C152HT, and GST-HT, respectively. Ubiquitylated species of GST-core proteins are marked by brackets. IB, immunoblot.

dilution assays. Exogenous expression of E6AP reduced the supernatant infectivity titer, whereas inactive E6AP had no effect on its infectivity titer (Fig. 9D), suggesting that the E6AP-dependent ubiquitin proteasome pathway affects the production of HCV particles through downregulation of the core protein.

E6AP silencing increases the levels of intracellular HCV core protein and supernatant infectivity titers in HCV-infected Huh-7 cells. Finally, to further validate the role of E6AP in HCV production, expression of endogenous E6AP was knocked down by siRNA and the HCV infectivity titers released from HCV JFH1-infected cells were examined. Knockdown of E6AP by siRNA led to an increase in intracellular core protein levels (Fig. 10A) and supernatant HCV infectivity titers (Fig. 10B). Taken together, our results suggest that E6AP mediates ubiquitylation and degradation of HCV core protein in HCV-infected cells, thereby affecting the production of HCV particles.

DISCUSSION

HCV core protein is a major component of viral nucleocapsid, plays a central role in viral assembly (25, 40), and contributes to viral pathogenesis and hepatocarcinogenesis (9). Therefore, it is important to clarify the molecular mechanisms that govern the cellular stability of this viral protein. We have previously reported that processing at the C-terminal hydrophobic domain of the core protein leads to efficient polyubiquitylation of the core protein (52). In this study, we identified E6AP as an HCV core-binding protein and showed that HCV core protein interacts with E6AP in vivo and in vitro, that E6AP enhances ubiquitylation and degradation of the mature core protein as well as the C-terminally truncated core protein, and that HCV core protein expressed from infectious HCV is degraded via E6AP-dependent proteolysis. HCV core protein and E6AP were found to colocalize in the cytoplasm, especially in the perinuclear region. Moreover, exogenous expression of E6AP reduces intracellular core protein levels and supernatant HCV infectivity titers in HCV-infected Huh-7 cells. Knockdown of endogenous E6AP by siRNA increases intracellular core protein levels and supernatant infectivity titers in HCV-infected cells. These findings suggest that E6AP mediates ubiquitylation and degradation of HCV core protein, thereby affecting the production of HCV particles.

HCV core protein interacts with E6AP through the region of the core protein between aa 58 and aa 71. These 14 amino acids are highly conserved, with the first nine amino acids (PRGRRQPIP) present in the core protein of all the HCV genotypes (3). This result suggests that E6AP-dependent degradation of HCV core protein is common to all HCV genotypes and plays an important role in the HCV life cycle or viral pathogenesis. Our data indicated that HCV core proteins of genotypes 1b and 2a are subjected to proteolysis through an E6AP-mediated degradation pathway. We are currently examining whether E6AP promotes degradation of HCV core proteins of other genotypes.

Studies in addition to ours have reported that other HCV proteins, such as NS5B (8), the unglycosylated cytosolic form of E2 (39), NS2 (7), and F protein (58), are degraded through the ubiquitin-proteasome pathway. These studies suggest that the ubiquitin-proteasome pathway plays a role in the HCV life cycle or viral pathogenesis. To our knowledge, the present study is the first to demonstrate that the ubiquitin-proteasome pathway affects the HCV life cycle.

PA28γ was found to interact with HCV core protein in hepatocytes and promote proteasomal degradation of HCV core protein (30). PA28γ, however, has been shown to function

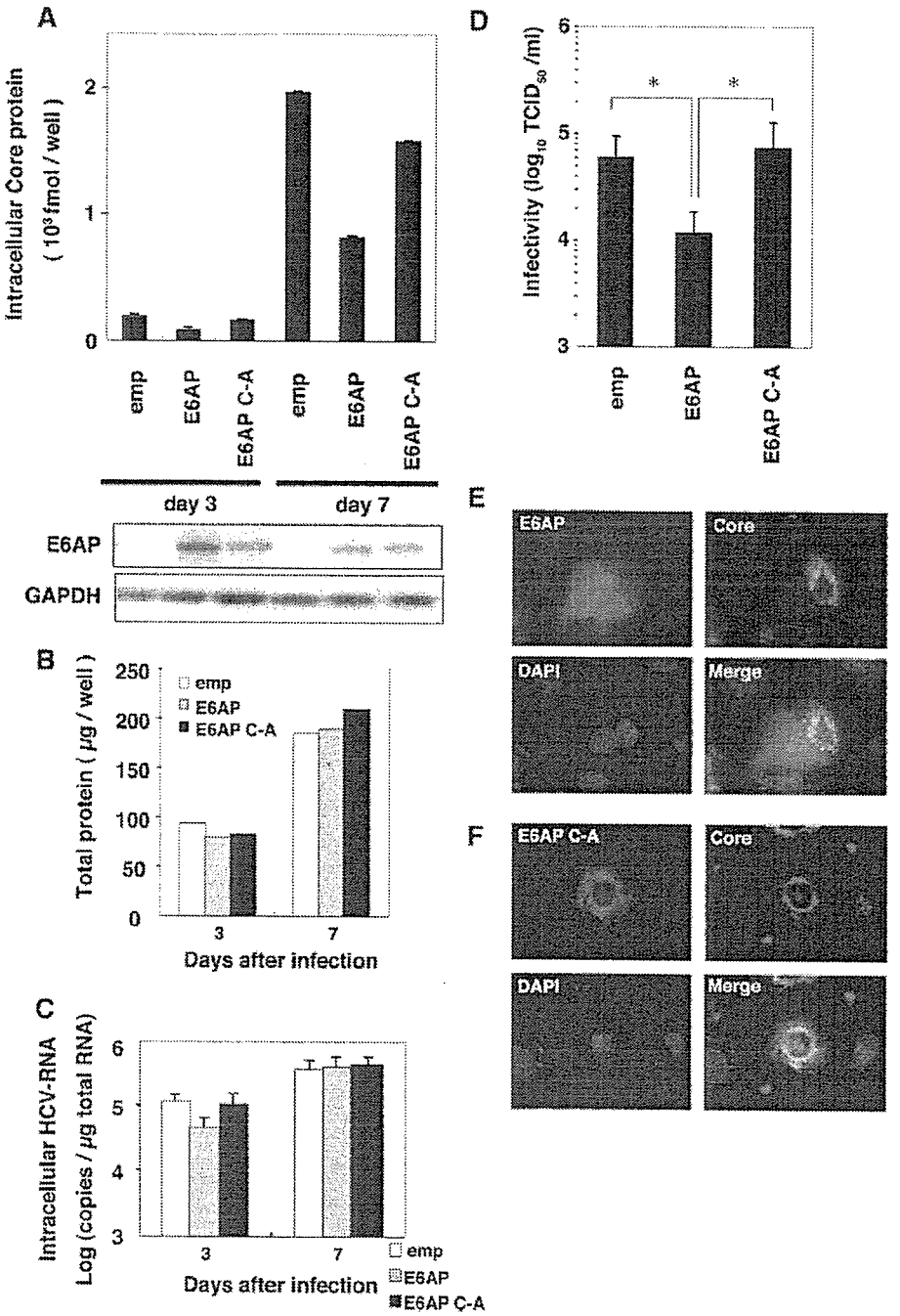

FIG. 9. Exogenous expression of E6AP reduces intracellular HCV core protein levels and supernatant infectivity titers in HCV-infected Huh-7 cells. Naïve Huh-7 cells were seeded as described in Materials and Methods; inoculated with 2.5 ml of the inoculum including infectious HCV JFH1 (6.5×10^5 $TCID_{50}$/ml); and transfected with 6 μg of empty plasmid, pCAG-HA-E6AP, or pCAG-HA-E6AP C-A. The culture supernatant and the cells were collected at days 3 and 7 postinfection. (A) Intracellular HCV core protein levels. (B) Levels of total protein. (C) Levels of intracellular HCV RNA in HCV-infected Huh-7 cells. Data represent the averages of three experiments with error bars. (D) Supernatant infectivity titers. At day 7 postinfection, culture supernatants were collected and assayed for $TCID_{50}$ determinations. The difference between empty vector and E6AP or between E6AP and E6AP C-A was significant (*, $P < 0.05$, Student's t test). (E and F) HCV JFH1-infected Huh-7 cells were transfected with either MEF-E6AP plasmid or MEF-E6AP C-A plasmid, grown on coverslips, fixed, and processed for double-label immunofluorescence for HCV core and MEF-E6AP (E) or MEF-E6AP C-A (F). Anticore MAb (2H9) and anti-FLAG PAb were used as primary antibodies. Nuclei were visualized by staining the cells with DAPI. All the samples were examined with a BZ-8000 microscope. Representative images of individual cells are shown with merge images. emp, empty vector.

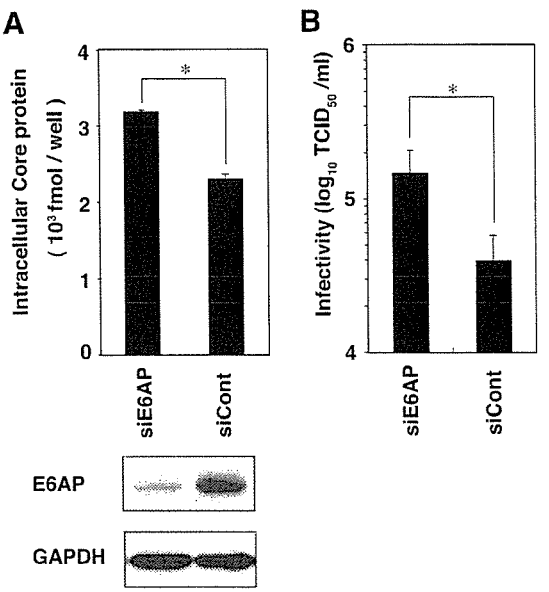

FIG. 10. E6AP silencing leads to an increase in the level of intracellular HCV core protein and supernatant infectivity titer in HCV-infected Huh-7 cells. (A) HCV JFH1-infected cells were replated in a six-well plate at 3×10^5 cells/well and transfected with 40 pmol of E6AP siRNA or control siRNA. The culture medium was changed at 24 h after transfection. The cells were harvested at day 2 after transfection, and the intracellular core protein levels were quantitated using the HCV core antigen ELISA. Equivalent amounts of the whole-cell lysates were separated by SDS-PAGE and analyzed by immunoblotting with anti-E6AP MAb or anti-GAPDH MAb. (B) Culture supernatants were collected at day 2 after transfection and assayed for $TCID_{50}$ determinations. For both panels, the difference between E6AP siRNA and control siRNA was significant (*, $P < 0.05$, Student's t test).

in a ubiquitin-independent, ATP-independent, and 20S proteasome-dependent pathway (27). There have been reports that several cellular factors, such as p53 (2), p73 (2), and RPN4 (18), are degraded through two alternative pathways, the ubiquitin-dependent 26S proteasome-dependent pathway and the ubiquitin-independent 20S proteasome-dependent pathway. Here we provide evidence that E6AP mediates ubiquitylation of HCV core protein. Still unclear is whether the PA28γ-dependent pathway requires polyubiquitylation of HCV core protein. HCV core protein is predominantly localized in the cytoplasm, especially at the endoplasmic reticulum membrane, on the surface of lipid droplets, and on mitochondria and mitochondrion-associated membranes (51). In HCV JFH1-infected cells, HCV core was found to localize in the cytoplasm and frequently to accumulate in the perinuclear region and the lipid droplets (44). Our results indicated that E6AP colocalized with HCV core protein especially in the perinuclear region. PA28γ was found to colocalize with HCV core protein in the nucleus. Functional differences may exist between the E6AP-dependent pathway and the PA28γ-dependent pathway in the stability control of HCV core protein. The functional role of the E6AP-dependent pathway and the PA28γ-dependent pathway remains to be elucidated.

The HCV core-binding region of E6AP was mapped to the region between aa 418 and aa 517. The multicopy maintenance protein 7, Mcm7, interacts with E6AP through a short motif, termed the L2G box (aa 412 to 414), that lies within the E6 binding site of E6AP (23). Our data indicated that the E6 binding region containing the L2G motif is not required for interaction between HCV core protein and E6AP (Fig. 2C, lane M).

We propose here that E6AP may affect the production of HCV particles through controlling the amounts of HCV core protein. This mechanism may contribute to persistent infection. The E6AP binding domain of the core protein resides in the RNA-binding domain and binding domains for many host factors (40). These factors may affect the binding between E6AP and HCV core protein, resulting in control of E6AP-dependent core degradation. Another possibility is that HCV core protein may affect the normal function of E6AP, thereby contributing to pathogenesis. It will be intriguing to investigate whether HCV core protein has any effect on E6AP-dependent degradation of host factors. The other intriguing possibility is that HCV core-E6AP complex may function as an E3 ligase-like E6-E6AP complex to target host factors for proteasomal degradation and contribute to viral pathogenesis.

In conclusion, we have demonstrated that E6AP interacts with HCV core protein in vitro and in vivo and mediates ubiquitin-dependent degradation of the core protein, leading to downregulation of HCV particles. We propose that the E6AP-mediated ubiquitin-proteasome pathway may play a role in affecting the production of HCV particles through controlling the amounts of viral nucleocapsid protein. Identification of the specific E3 ubiquitin ligase may contribute to gaining a better understanding of the biology of the HCV life cycle as well as molecular details of the ubiquitin-dependent degradation of HCV core protein.

ACKNOWLEDGMENTS

We thank D. Bohmann (EMBL) for providing pMT123, K. Miyazono (University of Tokyo) for pcDEF3-6Myc-WWP1, and K. Iwai (Osaka City University) for recombinant baculovirus carrying His 6-mouse E1. Huh-7.5.1 cells and Huh-7 cells were kindly provided by F. V. Chisari (Scripps Research Institute). We also thank P. Zhou (Weill Medical College of Cornell University), S. I. Wells (Cincinnati Children's Hospital Medical Center), and A. W. Hudson (Medical College of Wisconsin) for critical readings of the manuscript; M. Matsuda, S. Yoshizaki, M. Ikeda, and M. Sasaki for technical assistance; Y. Sugiyama and S. Senzui for plasmid construction; and T. Mizoguchi for secretarial work.

This work was supported in part by a grant for Research on Health Sciences focusing on Drug Innovation from the Japan Health Sciences Foundation; by grants-in-aid from the Ministry of Health, Labor and Welfare; by grants-in-aid from the Ministry of Education, Culture, Sports, Science and Technology; and by the program for Promotion of Fundamental Studies in Health Sciences of the National Institute of Biomedical Innovation (NIBIO), Japan. T.I. was supported in part by a grant from Novartis Foundation (Japan) for the Promotion of Science and by the Tokyo Metropolitan University President's Fund, Special Emphasis Research Project of Japan.

REFERENCES

1. **Aizaki, H., Y. Aoki, T. Harada, K. Ishii, T. Suzuki, S. Nagamori, G. Toda, Y. Matsuura, and T. Miyamura.** 1998. Full-length complementary DNA of hepatitis C virus genome from an infectious blood sample. Hepatology **27**: 621–627.
2. **Asher, G., P. Tsvetkov, C. Kahana, and Y. Shaul.** 2005. A mechanism of ubiquitin-independent proteasomal degradation of the tumor suppressors p53 and p73. Genes Dev. **19**:316–321.
3. **Bukh, J., R. H. Purcell, and R. H. Miller.** 1994. Sequence analysis of the core gene of 14 hepatitis C virus genotypes. Proc. Natl. Acad. Sci. USA **91**:8239–8243.

4. **Chen, C., and H. Okayama.** 1987. High-efficiency transformation of mammalian cells by plasmid DNA. Mol. Cell. Biol. **7**:2745–2752.
5. **Choo, Q. L., G. Kuo, A. J. Weiner, L. R. Overby, D. W. Bradley, and M. Houghton.** 1989. Isolation of a cDNA clone derived from a blood-borne non-A, non-B viral hepatitis genome. Science **244**:359–362.
6. **Choo, Q. L., K. H. Richman, J. H. Han, K. Berger, C. Lee, C. Dong, C. Gallegos, D. Coit, R. Medina-Selby, P. J. Barr, et al.** 1991. Genetic organization and diversity of the hepatitis C virus. Proc. Natl. Acad. Sci. USA **88**:2451–2455.
7. **Franck, N., J. Le Seyec, C. Guguen-Guillouzo, and L. Erdtmann.** 2005. Hepatitis C virus NS2 protein is phosphorylated by the protein kinase CK2 and targeted for degradation to the proteasome. J. Virol. **79**:2700–2708.
8. **Gao, L., H. Tu, S. T. Shi, K. J. Lee, M. Asanaka, S. B. Hwang, and M. M. Lai.** 2003. Interaction with a ubiquitin-like protein enhances the ubiquitination and degradation of hepatitis C virus RNA-dependent RNA polymerase. J. Virol. **77**:4149–4159.
9. **Giannini, C., and C. Brechot.** 2003. Hepatitis C virus biology. Cell Death Differ. **10**(Suppl. 1):S27–S38.
10. **Grakoui, A., D. W. McCourt, C. Wychowski, S. M. Feinstone, and C. M. Rice.** 1993. Characterization of the hepatitis C virus-encoded serine proteinase: determination of proteinase-dependent polyprotein cleavage sites. J. Virol. **67**:2832–2843.
11. **Harris, K. F., I. Shoji, E. M. Cooper, S. Kumar, H. Oda, and P. M. Howley.** 1999. Ubiquitin-mediated degradation of active Src tyrosine kinase. Proc. Natl. Acad. Sci. USA **96**:13738–13743.
12. **Hijikata, M., H. Mizushima, T. Akagi, S. Mori, N. Kakiuchi, N. Kato, T. Tanaka, K. Kimura, and K. Shimotohno.** 1993. Two distinct proteinase activities required for the processing of a putative nonstructural precursor protein of hepatitis C virus. J. Virol. **67**:4665–4675.
13. **Huibregtse, J. M., M. Scheffner, S. Beaudenon, and P. M. Howley.** 1995. A family of proteins structurally and functionally related to the E6-AP ubiquitin-protein ligase. Proc. Natl. Acad. Sci. USA **92**:2563–2567.
14. **Huibregtse, J. M., M. Scheffner, and P. M. Howley.** 1993. Cloning and expression of the cDNA for E6-AP, a protein that mediates the interaction of the human papillomavirus E6 oncoprotein with p53. Mol. Cell. Biol. **13**:775–784.
15. **Hussy, P., H. Langen, J. Mous, and H. Jacobsen.** 1996. Hepatitis C virus core protein: carboxy-terminal boundaries of two processed species suggest cleavage by a signal peptide peptidase. Virology **224**:93–104.
16. **Ichimura, T., H. Yamamura, K. Sasamoto, Y. Tominaga, M. Taoka, K. Kakiuchi, T. Shinkawa, N. Takahashi, S. Shimada, and T. Isobe.** 2005. 14-3-3 proteins modulate the expression of epithelial Na^+ channels by phosphorylation-dependent interaction with Nedd4-2 ubiquitin ligase. J. Biol. Chem. **280**:13187–13194.
17. **Iwai, K., K. Yamanaka, T. Kamura, N. Minato, R. C. Conaway, J. W. Conaway, R. D. Klausner, and A. Pause.** 1999. Identification of the von Hippel-Lindau tumor-suppressor protein as part of an active E3 ubiquitin ligase complex. Proc. Natl. Acad. Sci. USA **96**:12436–12441.
18. **Ju, D., and Y. Xie.** 2004. Proteasomal degradation of RPN4 via two distinct mechanisms, ubiquitin-dependent and -independent. J. Biol. Chem. **279**: 23851–23854.
19. **Kao, W. H., S. L. Beaudenon, A. L. Talis, J. M. Huibregtse, and P. M. Howley.** 2000. Human papillomavirus type 16 E6 induces self-ubiquitination of the E6AP ubiquitin-protein ligase. J. Virol. **74**:6408–6417.
20. **Kato, T., M. Miyamoto, A. Furusaka, T. Date, K. Yasui, J. Kato, S. Matsushima, T. Komatsu, and T. Wakita.** 2003. Processing of hepatitis C virus core protein is regulated by its C-terminal sequence. J. Med. Virol. **69**:357–366.
21. **Kishino, T., M. Lalande, and J. Wagstaff.** 1997. UBE3A/E6-AP mutations cause Angelman syndrome. Nat. Genet. **15**:70–73.
22. **Komuro, A., T. Imamura, M. Saitoh, Y. Yoshida, T. Yamori, K. Miyazono, and K. Miyazawa.** 2004. Negative regulation of transforming growth factor-beta (TGF-beta) signaling by WW domain-containing protein 1 (WWP1). Oncogene **23**:6914–6923.
23. **Kuhne, C., and L. Banks.** 1998. E3-ubiquitin ligase/E6-AP links multicopy maintenance protein 7 to the ubiquitination pathway by a novel motif, the L2G box. J. Biol. Chem. **273**:34302–34309.
24. **Kumar, S., A. L. Talis, and P. M. Howley.** 1999. Identification of HHR23A as a substrate for E6-associated protein-mediated ubiquitination. J. Biol. Chem. **274**:18785–18792.
25. **Kunkel, M., M. Lorinczi, R. Rijnbrand, S. M. Lemon, and S. J. Watowich.** 2001. Self-assembly of nucleocapsid-like particles from recombinant hepatitis C virus core protein. J. Virol. **75**:2119–2129.
26. **Kuo, G., Q. L. Choo, H. J. Alter, G. L. Gitnick, A. G. Redeker, R. H. Purcell, T. Miyamura, J. L. Dienstag, M. J. Alter, C. E. Stevens, et al.** 1989. An assay for circulating antibodies to a major etiologic virus of human non-A, non-B hepatitis. Science **244**:362–364.
27. **Li, X., D. M. Lonard, S. Y. Jung, A. Malovannaya, Q. Feng, J. Qin, S. Y. Tsai, M. J. Tsai, and B. W. O'Malley.** 2006. The SRC-3/AIB1 coactivator is degraded in a ubiquitin- and ATP-independent manner by the REGγ proteasome. Cell **124**:381–392.
28. **Lindenbach, B. D., M. J. Evans, A. J. Syder, B. Wolk, T. L. Tellinghuisen, C. C. Liu, T. Maruyama, R. O. Hynes, D. R. Burton, J. A. McKeating, and C. M. Rice.** 2005. Complete replication of hepatitis C virus in cell culture. Science **309**:623–626.
29. **McLauchlan, J., M. K. Lemberg, G. Hope, and B. Martoglio.** 2002. Intramembrane proteolysis promotes trafficking of hepatitis C virus core protein to lipid droplets. EMBO J. **21**:3980–3988.
30. **Moriishi, K., T. Okabayashi, K. Nakai, K. Moriya, K. Koike, S. Murata, T. Chiba, K. Tanaka, R. Suzuki, T. Suzuki, T. Miyamura, and Y. Matsuura.** 2003. Proteasome activator PA28γ-dependent nuclear retention and degradation of hepatitis C virus core protein. J. Virol. **77**:10237–10249.
31. **Moriya, K., H. Fujie, Y. Shintani, H. Yotsuyanagi, T. Tsutsumi, K. Ishibashi, Y. Matsuura, S. Kimura, T. Miyamura, and K. Koike.** 1998. The core protein of hepatitis C virus induces hepatocellular carcinoma in transgenic mice. Nat. Med. **4**:1065–1067.
32. **Moriya, K., H. Yotsuyanagi, Y. Shintani, H. Fujie, K. Ishibashi, Y. Matsuura, T. Miyamura, and K. Koike.** 1997. Hepatitis C virus core protein induces hepatic steatosis in transgenic mice. J. Gen. Virol. **78**:1527–1531.
33. **Natsume, T., Y. Yamauchi, H. Nakayama, T. Shinkawa, M. Yanagida, N. Takahashi, and T. Isobe.** 2002. A direct nanoflow liquid chromatography-tandem mass spectrometry system for interaction proteomics. Anal. Chem. **74**:4725–4733.
34. **Niwa, H., K. Yamamura, and J. Miyazaki.** 1991. Efficient selection for high-expression transfectants with a novel eukaryotic vector. Gene **108**:193–199.
35. **Oda, H., S. Kumar, and P. M. Howley.** 1999. Regulation of the Src family tyrosine kinase Blk through E6AP-mediated ubiquitination. Proc. Natl. Acad. Sci. USA **96**:9557–9562.
36. **Ogino, T., H. Fukuda, S. Imajoh-Ohmi, M. Kohara, and A. Nomoto.** 2004. Membrane binding properties and terminal residues of the mature hepatitis C virus capsid protein in insect cells. J. Virol. **78**:11766–11777.
37. **Okamoto, K., K. Moriishi, T. Miyamura, and Y. Matsuura.** 2004. Intramembrane proteolysis and endoplasmic reticulum retention of hepatitis C virus core protein. J. Virol. **78**:6370–6380.
38. **Owsianka, A. M., and A. H. Patel.** 1999. Hepatitis C virus core protein interacts with a human DEAD box protein DDX3. Virology **257**:330–340.
39. **Pavio, N., D. R. Taylor, and M. M. Lai.** 2002. Detection of a novel unglycosylated form of hepatitis C virus E2 envelope protein that is located in the cytosol and interacts with PKR. J. Virol. **76**:1265–1272.
40. **Polyak, S. J., K. C. Klein, I. Shoji, T. Miyamura, and J. R. Lingappa.** 2006. Assemble and interact: pleiotropic functions of the HCV core protein, p. 89–119. *In* S.-L. Tan (ed.), Hepatitis C viruses: genomes and molecular biology. Horizon Bioscience, Norwich, United Kingdom.
41. **Poynard, T., M. F. Yuen, V. Ratziu, and C. L. Lai.** 2003. Viral hepatitis C. Lancet **362**:2095–2100.
42. **Ravaggi, A., G. Natoli, D. Primi, A. Albertini, M. Levrero, and E. Cariani.** 1994. Intracellular localization of full-length and truncated hepatitis C virus core protein expressed in mammalian cells. J. Hepatol. **20**:833–836.
43. **Ray, R. B., L. M. Lagging, K. Meyer, and R. Ray.** 1996. Hepatitis C virus core protein cooperates with *ras* and transforms primary rat embryo fibroblasts to tumorigenic phenotype. J. Virol. **70**:4438–4443.
44. **Rouille, Y., F. Helle, D. Delgrange, P. Roingeard, C. Voisset, E. Blanchard, S. Belouzard, J. McKeating, A. H. Patel, G. Maertens, T. Wakita, C. Wychowski, and J. Dubuisson.** 2006. Subcellular localization of hepatitis C virus structural proteins in a cell culture system that efficiently replicates the virus. J. Virol. **80**:2832–2841.
45. **Saito, I., T. Miyamura, A. Ohbayashi, H. Harada, T. Katayama, S. Kikuchi, Y. Watanabe, S. Koi, M. Onji, Y. Ohta, et al.** 1990. Hepatitis C virus infection is associated with the development of hepatocellular carcinoma. Proc. Natl. Acad. Sci. USA **87**:6547–6549.
46. **Santolini, E., G. Migliaccio, and N. La Monica.** 1994. Biosynthesis and biochemical properties of the hepatitis C virus core protein. J. Virol. **68**: 3631–3641.
47. **Sato, S., M. Fukasawa, Y. Yamakawa, T. Natsume, T. Suzuki, I. Shoji, H. Aizaki, T. Miyamura, and M. Nishijima.** 2006. Proteomic profiling of lipid droplet proteins in hepatoma cell lines expressing hepatitis C virus core protein. J. Biochem. (Tokyo) **139**:921–930.
48. **Scheffner, M., J. M. Huibregtse, and P. M. Howley.** 1994. Identification of a human ubiquitin-conjugating enzyme that mediates the E6-AP-dependent ubiquitination of p53. Proc. Natl. Acad. Sci. USA **91**:8797–8801.
49. **Scheffner, M., J. M. Huibregtse, R. D. Vierstra, and P. M. Howley.** 1993. The HPV-16 E6 and E6-AP complex functions as a ubiquitin-protein ligase in the ubiquitination of p53. Cell **75**:495–505.
50. **Scheffner, M., U. Nuber, and J. M. Huibregtse.** 1995. Protein ubiquitination involving an E1–E2-E3 enzyme ubiquitin thioester cascade. Nature **373**:81–83.
51. **Suzuki, R., S. Sakamoto, T. Tsutsumi, A. Rikimaru, K. Tanaka, T. Shimoike, K. Moriishi, T. Iwasaki, K. Mizumoto, Y. Matsuura, T. Miyamura, and T. Suzuki.** 2005. Molecular determinants for subcellular localization of hepatitis C virus core protein. J. Virol. **79**:1271–1281.
52. **Suzuki, R., K. Tamura, J. Li, K. Ishii, Y. Matsuura, T. Miyamura, and T. Suzuki.** 2001. Ubiquitin-mediated degradation of hepatitis C virus core pro-

tein is regulated by processing at its carboxyl terminus. Virology **280**:301–309.

53. **Suzuki, T., K. Omata, T. Satoh, T. Miyasaka, C. Arai, M. Maeda, T. Matsuno, and T. Miyamura.** 2005. Quantitative detection of hepatitis C virus (HCV) RNA in saliva and gingival crevicular fluid of HCV-infected patients. J. Clin. Microbiol. **43**:4413–4417.
54. **Takamizawa, A., C. Mori, I. Fuke, S. Manabe, S. Murakami, J. Fujita, E. Onishi, T. Andoh, I. Yoshida, and H. Okayama.** 1991. Structure and organization of the hepatitis C virus genome isolated from human carriers. J. Virol. **65**:1105–1113.
55. **Talis, A. L., J. M. Huibregtse, and P. M. Howley.** 1998. The role of E6AP in the regulation of p53 protein levels in human papillomavirus (HPV)-positive and HPV-negative cells. J. Biol. Chem. **273**:6439–6445.
56. **Wakita, T., T. Pietschmann, T. Kato, T. Date, M. Miyamoto, Z. Zhao, K. Murthy, A. Habermann, H. G. Krausslich, M. Mizokami, R. Bartenschlager, and T. J. Liang.** 2005. Production of infectious hepatitis C virus in tissue culture from a cloned viral genome. Nat. Med. **11**:791–796.
57. **Wertz, I. E., K. M. O'Rourke, Z. Zhang, D. Dornan, D. Arnott, R. J. Deshaies, and V. M. Dixit.** 2004. Human de-etiolated-1 regulates c-Jun by assembling a CUL4A ubiquitin ligase. Science **303**:1371–1374.
58. **Xu, Z., J. Choi, W. Lu, and J. Ou.** 2003. Hepatitis C virus F protein is a short-lived protein associated with the endoplasmic reticulum. J. Virol. **77**: 1578–1583.
59. **Yamaguchi, R., S. Momosaki, G. Gao, C. C. Hsia, M. Kojiro, C. Scudamore, and E. Tabor.** 2004. Truncated hepatitis C virus core protein encoded in hepatocellular carcinomas. Int. J. Mol. Med. **14**:1097–1100.
60. **Yasui, K., T. Wakita, K. Tsukiyama-Kohara, S. I. Funahashi, M. Ichikawa, T. Kajita, D. Moradpour, J. R. Wands, and M. Kohara.** 1998. The native form and maturation process of hepatitis C virus core protein. J. Virol. **72**:6048–6055.
61. **Zhong, J., P. Gastaminza, G. Cheng, S. Kapadia, T. Kato, D. R. Burton, S. F. Wieland, S. L. Uprichard, T. Wakita, and F. V. Chisari.** 2005. Robust hepatitis C virus infection in vitro. Proc. Natl. Acad. Sci. USA **102**:9294–9299.

JOURNAL OF VIROLOGY, Sept. 2004, p. 9713–9720 Vol. 78, No. 18
0022-538X/04/$08.00+0 DOI: 10.1128/JVI.78.18.9713–9720.2004

Regulation of Hepatitis C Virus Replication by Interferon Regulatory Factor 1

Nobuhiko Kanazawa,[1]† Masayuki Kurosaki,[1]†‡ Naoya Sakamoto,[1]* Nobuyuki Enomoto,[1,2] Yasuhiro Itsui,[1] Tsuyoshi Yamashiro,[1] Yoko Tanabe,[1] Shinya Maekawa,[1] Mina Nakagawa,[1] Cheng-Hsin Chen,[1] Sei Kakinuma,[1] Shigeru Oshima,[1] Tetsuya Nakamura,[1] Takanobu Kato,[3] Takaji Wakita,[3] and Mamoru Watanabe[1]

Department of Gastroenterology and Hepatology, Tokyo Medical and Dental University,[1] and Department of Microbiology, Tokyo Metropolitan Institute for Neuroscience,[3] Tokyo, and First Department of Internal Medicine, University of Yamanashi, Yamanashi,[2] Japan

Received 2 February 2004/Accepted 12 May 2004

Cellular antiviral responses are mediated partly by the expression of interferon-stimulated genes, triggered by viral genomes, their transcripts and replicative intermediates. Persistent replication of a hepatitis C virus (HCV) replicon suggests that the replicon does not elicit cellular innate antiviral responses. In the present study, we investigated regulatory factors of the interferon-mediated antiviral system in cells expressing an HCV replicon. Luciferase reporter assays revealed that the baseline activity of the interferon-stimulated response element (ISRE) was significantly lower in cells harboring the replicon than in naive cells. Among the proteins involved in the IFN/Jak/STAT pathway and in ISRE activity, the expression level of interferon regulatory factor 1 (IRF-1) was found to be significantly lower in cells harboring the replicon. Transfection of an IRF-1 expression construct into cells harboring the replicon caused an increase of ISRE activity, accompanied by suppression of expression of the HCV replicon. Moreover, in cured Huh7 cells from which the HCV replicon had been eliminated, the expression levels of IRF-1 and ISRE activity also were suppressed, demonstrating that the decrease of IRF-1 is attributable, not to active suppression by the viral proteins, but to adaptation of cells that enables replication of the HCV subgenome. The high permissiveness of the cured cells for the replicon was abolished by transgenic supplementation of IRF-1 expression. Taken together, IRF-1 is one of the key host factors that regulate intracellular HCV replication through modulation of interferon-stimulated-gene-mediated antiviral responses.

Hepatitis C virus (HCV) is one of the most important pathogens causing liver-related morbidity and mortality (3, 10). HCV establishes a persistent infection in the liver, leading to the development of chronic hepatitis, liver cirrhosis, and hepatocellular carcinoma. Interferon (IFN) plays a central role in eliminating HCV, not only following clinical therapeutic application but also as a cellular immune response (30, 39). Cellular innate responses to eliminate viruses are mediated by the IFN-stimulated genes (ISGs), including 2,5-oligoadenylate synthetase (OAS), double-stranded RNA-dependent protein kinase R, and MxA proteins, and by as-yet-uncharacterized genes (35). DNA microarray analyses of liver specimens from a chimpanzee infected with HCV revealed that the expression of various cytokines and chemokines is induced during the course of viral infection and its clearance and that a considerable proportion of the genes are induced by IFN-α or IFN-γ (5).

The control of expression of ISGs is directed by the IFN-stimulated response elements (ISRE) and/or IFN-γ-activated sites (GAS) located in their promoter and/or enhancer regions (30). GAS is the binding site for phosphorylated signal transducer and activator of transcription 1 (STAT1) homodimers called IFN-γ-activated factor (GAF), which in turn is activated through IFN-γ receptor-associated Janus kinase (Jak) (38). Thus, GAS drives the expression of genes induced by IFN-γ (11). On the other hand, ISRE is the binding site for the IFN-stimulated gene factor 3 (ISGF-3) that consists of phosphorylated STAT1 and STAT2, and IFN regulatory factor 9 (IRF-9) (38, 39). ISGF-3 is activated through the binding of IFN-α/β to their receptor (11).

Besides IFN receptor-mediated stimuli, other IRF family members regulate the expression levels of ISGs and IFN-α/β genes through binding to ISRE and a similar DNA sequence, positive regulatory domain (PRD) I, within the IFN-β promoter and PRD-like elements (PRD-LE) within IFN-α promoters (26, 27, 37, 38). These sequences respond differentially to each specific IRF—IRF-1, IRF-3, and IRF-7 in particular (26, 27, 37, 38). IRF-3 and IRF-7 have been identified as direct transducers of virus-mediated signaling and play a critical role in the induction of IFN genes (32, 33). Both IRF-3 and IRF-7, which reside in the cytoplasm, undergo virus-induced phosphorylation and translocate to the nucleus (38). IRF-7 can activate IFN-α and IFN-β genes through binding PRD-LE and PRDI, respectively, whereas IRF-3 predominantly affects the IFN-β gene and some ISGs through binding PRDI and ISRE, respectively (26, 31, 39). IRF-1 was first identified as a regulator of the promoter of the IFN-α/β gene (30). Cellular ex-

* Corresponding author. Mailing address: Department of Gastroenterology and Hepatology, Tokyo Medical and Dental University, 1-5-45 Yushima, Bunkyo-ku, Tokyo 113-8519, Japan. Phone: 81-3-5803-5877. Fax: 81-3-5803-0268. E-mail: nsakamoto.gast@tmd.ac.jp.
† N.K. and M.K. contributed equally to this work.
‡ Present address: Division of Gastroenterology and Hepatology, Musashino Red Cross Hospital, Tokyo, Japan.

pression of IRF-1 is induced by various cytokines, such as IFN-α/β/γ, tumor necrosis factor alpha, interleukin-1, interleukin-6, and LIF, and by viral infection (38). The recognition sequence of IRF-1, IRF-E, overlaps with that of ISRE, which binds ISGF-3 (37, 38). IRF-1 appears to function as a regulator of cellular antiviral responses to IFNs by affecting a set of ISGs. Overexpression of IRF-1 induces an antiviral state affecting various viruses, including vesicular stomatitis virus, encephalomyocarditis virus, and Newcastle disease virus (28).

Basic studies of HCV infection and replication were hampered by the lack of efficient cell culture systems. The HCV subgenomic replicon system, developed by Lohmann et al., is an efficient and noncytopathic cellular genomic replication model that has allowed various molecular studies of HCV replication (25). Host cells for the replicon generally are restricted to the human hepatoma cell line, Huh7. Furthermore, for continuous expression of the replicon, certain amino acid substitutions are required for adaptation to the host cells. In contrast, inoculation of these cellular adapted mutant HCV-RNAs into chimpanzee liver failed to induce persistent infection (9). These findings suggest that viral fitness to the host cellular environment is critical for the establishment of continuous replication.

In cells harboring the replicon, the expression of the replicon is abolished by small amounts of exogenous IFN-α/β/γ (6, 13, 16, 36), suggesting intact IFN receptor-mediated cellular antiviral responses. However, in the absence of IFN, persistent and high-level expression of the replicon makes us speculate that intracellular virus-induced antiviral responses are attenuated in the host cells or that those antiviral responses are suppressed by the expression of viral proteins.

In the present study, we investigated the factors associated with cellular antiviral responses and their regulation by IRFs and found that the baseline ISRE activity is decreased in cells expressing the HCV replicon, that the transcriptional decrease of IRF-1 is involved in the downregulation of the ISRE responses and, more importantly, that expression of IRF-1 negatively regulates HCV replication.

MATERIALS AND METHODS

Cell culture. Human hepatoma Huh7 cells were grown in conventional medium consisting of Dulbecco modified minimal essential medium (Sigma, St. Louis, Mo.) supplemented with 100 IU of penicillin/ml, 100 μg of streptomycin/ml, and 10% fetal bovine serum at 37°C under 5% CO_2. G418 (Wako, Osaka, Japan) was added to the culture medium to a final concentration of 200 μg/ml for cells carrying the HCV replicon.

Plasmid constructions. The plasmid, pHCV1bneo/delS is an HCV subgenomic replicon construct derived from the chimpanzee-infectious clone, HCV-N (GenBank accession no. AF139594, kindly provided by Christoph Seeger) (16). Another HCV-1b replicon construct, pR-J4/S2197P, is constructed from the HC-J4 clone (25a, 40). Both pHCV1bneo/delS and pR-J4/S2197P are bicistronic RNA molecules expressing the neomycin phosphotransferase (NPT) gene and the HCV nonstructural genes spanning from NS3 to NS5B. Plasmid pRep-Feo was derived from pHCV1bneo/delS with replacement of the NPT gene by a fusion of the firefly luciferase (Fluc) and NPT genes (36, 41). pRep-Fluc was constructed from pHCV1bneo/delS by replacing the NPT gene with the firefly luciferase gene for transient-replication assay. A replication-defective replicon construct, pRep-Fluc-NS5Bdel, was constructed from pHC1bneo/delS by introducing a frameshift mutation into NS5B by BclI digestion and served as a replication-negative control.

The full-length human IRF-1 gene was amplified by PCR from human intestine and cloned into pcDNA3 and pcDNA4/TO/myc-His B (Invitrogen, Carlsbad, Calif.) to yield the mammalian expression construct, pcDNA3-IRF-1 and pcDNA4/to/IRF-1-Myc/His. The nucleotide sequence was confirmed. pISRE-TA-Luc (Invitrogen) contained five copies of consensus ISRE motifs upstream of the firefly luciferase gene. pGAS-TA-Luc (Invitrogen) contained two copies of the STAT1 enhancer element upstream of the firefly luciferase gene. pTA-Luc (Invitrogen), which lacks the enhancer element, was used for background determination. pcDNA3.1 (Invitrogen) was used as an empty vector for mock transfection. pRL-CMV (Promega, Madison, Wis.), which expresses the *Renilla* luciferase protein, was used for correction of transfection efficiency.

In vitro transcription. The replicon RNA was synthesized in vitro from 1 μg of linearized replicon plasmid by the RiboMax Large Scale RNA Production System (Promega) by using T7 RNA polymerase. After DNase I treatment, the transcribed RNA was purified by the acid guanidinium thiocyanate-phenol-chloroform method with ISOGEN (Nippon Gene, Tokyo, Japan) to remove completely trace amounts of residual template DNA, and resuspended in RNase-free water.

Electroporation and G418 selection to obtain cells harboring the HCV replicon. Subconfluent Huh7 cells were treated with trypsin, and 5×10^6 cells were resuspended in 500 μl of serum-free Dulbecco modified Eagle medium-F12 medium (Sigma) in the presence of 10 μg of each replicon RNA, transferred to a 4-mm electroporation cuvette (Equi Bio, Middlesex, United Kingdom), and subjected to an electric pulse (1,050 μF and 270 V) by using the EasyJect system (Equi Bio). After electroporation, the cell suspension was diluted with conventional medium and plated in 10-cm-diameter cell culture dishes. After 24 h, G418 was added to a concentration of 200 μg/ml, and the medium was changed twice weekly. At 3 weeks after transfection, G418-resistant colonies appeared, and cell lines harboring continuous replication of the replicon were established. Cell lines Huh7/Rep-N, Huh7/Rep-J4, and Huh7/Rep-Feo were established from HCV1bneo/delS, R-J4/S2197P, and Rep-Feo, respectively.

Establishment of cured Huh7 cells. Cured Huh7 cells, from which the replicon had been eliminated, were established by treating Huh7/Rep-Feo cells with 100 U of IFN-α/ml for 14 days. Clearance of replicon RNA was confirmed by reverse transcription-PCR (RT-PCR) and by the loss of resistance to G418.

Electroporation and transient-replication assays. Subconfluent cells were treated with trypsin, and 6×10^6 cells were resuspended in 500 μl of OPTI-MEM in the presence of 5 μg of luciferase-expressing replicon RNA Rep-Fluc and were electroporated as described above. After electroporation, the cell suspension was diluted to 12 ml with conventional medium and seeded onto a 24-well plate. The luciferase activities of the cell lysates were measured by using a single luciferase assay protocol. To correct the efficiency of induction, each value was shown as a relative ratio adjusted by a value at 4 h of electroporation.

Transient transfection. Transient transfection was performed by using FuGENE-6 transfection reagent (Roche Applied Science, Indianapolis, Ind.) and Lipofectamine 2000 (Invitrogen) according to the manufacturer's protocol.

Reporter assays. To measure the ISRE and GAS activity, cells were seeded at 5×10^4 per well in 24-well plates on the day before transfection. Totals of 400 ng of pISRE-TA-Luc, pGAS-TA-Luc, or pTA-Luc with 1 ng of pRL-CMV were transfected to each well by using 2 μl of Lipofectamine 2000. At 48 h after transfection, dual luciferase assays were performed on the cell lysates. To determine the efficacy of IFN on ISRE activities, the 6-h treatment of IFN-α was made 48 h after the transfection of pISRE-TA-Luc and pRL-CMV. A reporter assay was performed to determine the effect of IRF-1 on ISRE in the cells harboring the replicon. A total of 5×10^4 Huh7/Rep-N cells per well was subcultured onto 24-well plates the day before transfection. A total of 100 ng of pISRE-TA-Luc and various amounts of pcDNA3-IRF-1 with empty vector and 0.1 ng of pRL-CMV, to a total mass of DNA of 400 ng, were transfected by using 2 μl of Lipofectamine 2000. At 48 h after transfection, dual luciferase assays were performed on the cell lysates.

Transfection of pcDNA3-IRF-1 to Huh7/Feo was performed to determine the effect of IRF-1 on the replication of the HCV replicon. A total of 5×10^4 Huh7/Rep-Feo cells per well were subcultured onto 24-well plates, and various amounts of pcDNA3-IRF-1 with empty vector, to a total mass of DNA of 400 ng, were transfected to each well by using 1.2 μl of FuGENE-6. At 48 h after transfection, the cell lysates were collected and single luciferase assays were performed. Luciferase activities were quantified with a luminometer (TD-20/20; Turner Designs, Sunnyvale, Calif.) by using the dual-luciferase reporter assay system (Promega) for dual luciferase assay and the Bright-Glo luciferase assay system (Promega) for single luciferase assay.

RT-PCR and LightCycler-based PCR assay. Total cellular RNA was extracted from cells by using ISOGEN. Then, 2 μg of total cellular RNA was used to generate cDNA from each sample by using SuperScript II (Invitrogen) reverse transcriptase. The mRNA expression levels were measured with the LightCycler PCR and detection system (Roche). Thermocycling was done in a final volume of 10 μl containing 1 μl of cDNA sample or calibrator, 1.25 mM $MgCl_2$, 0.5 μM concentrations of each primer, and 1 μl of LightCycler FastStart DNA Master

SYBR Green 1 mix (Roche). Cycle numbers of the logarithmic linear phase were plotted against the logarithm of the concentration of template DNA. The concentrations of DNA in the samples were calculated by comparing the cycle numbers of the logarithmic linear phase of the samples with the external standards. The results of amplification of the samples were verified on a 1% agarose gel. No nonspecific amplification product was documented. The primers used were as follows: IRF-1 sense (positions 1018 to 1043; 5′-GTAAGGAGGAGCCAGAA ATTGACAGC-3′), IRF-1 antisense (positions 1152 to 1175; 5′-CTACGGTGC ACAGGGAATGGCCTG-3′), IRF-3 sense (positions 1154 to 1177; 5′-ACGTG CCTCAGGGCCTTGGTAGAA-3′), IRF-3 antisense (positions 1307 to 1330; 5′-TCAGCTCTCCCCAGGGCCCTGGAA-3′), STAT1-α/β sense (positions 2291 to 2320; 5′-ACTGGATATATCAAGACTGAGTTGATTTCT-3′), STAT1-α antisense (positions 2411 to 2440; 5′-GTTCATCATACTGTCGAATTCTACAGA GCC-3′), STAT1-β antisense (positions 2411 to 2440; 5′-GATAGCAATTACA ATGGAAAAGTAAAATAC-3′), β-actin sense (positions 1011 to 1040; 5′-AC AATGAAGATCAAGATCATTGCTCCTCCT-3′), and β-actin antisense (positions 1131 to 1160; 5′-TTTGCGGTGGACGATGGAGGGGCCGGACTC-3′).

Preparation of siRNA and transfection. Sense and antisense strands of small interfering RNA (siRNA) oligonucleotides directed against IRF-1 mRNA were synthesized. The sequences were 5′-CCAAGAACCAGAGAAAAGAdTdT-3′ (sense) and 5′-UCUUUUCUCUGGUUCUUGGdTdT-3′ (antisense). siRNA directed against an unrelated target was used as a negative control.

MTS assays. To evaluate cell growth and cell viability, dimethylthiazol carboxymethoxyphenyl sulfophenyl tetrazolium (MTS) assays were performed by using the CellTiter 96 AQueous One-Solution cell proliferation assay (Promega).

Preparation of nuclear extracts. After two washes in ice-cold phosphate-buffered saline, 2×10^7 cells were harvested and centrifuged at $1,000 \times g$ for 5 min in a microcentrifuge. The cell pellet was resuspended in 80 μl of buffer A (10 mM Tris-HCl [pH 7.3], 1.5 mM $MgCl_2$, 10 mM KCl, 1 mM dithiothreitol, 0.4% Nonidet P-40, 1 mM phenylmethylsulfonyl fluoride, 10 μg of aprotinin/ml, 1 μM pepstatin, 50 mM NaF, and 1 mM Na_3VO_4). After incubation on ice for 5 min, cell lysates were centrifuged, and the nuclear pellet was then resuspended in 75 μl of buffer C (20 mM Tris-HCl [pH 7.3], 1.5 mM $MgCl_2$, 484 mM KCl, 1 mM dithiothreitol, 0.2 mM EDTA, 25% glycerol, 1 mM phenylmethylsulfonyl fluoride, 10 μg of aprotinin/ml, 1 μM pepstatin, 50 mM NaF, and 1 mM Na_3VO_4), followed by incubation for 30 min at 4°C. Nuclear debris were pelleted with centrifugation at $12,000 \times g$ for 15 min, and the supernatant was used as nuclear extracts (26a).

Western blot analysis. A total of 25 μg of nuclear extract lysate was electrophoresed through a NuPAGE 10% Bis-Tris gel (Invitrogen) and blotted onto the polyvinylidene difluoride Western blot membranes (Roche). The membranes were incubated with rabbit polyclonal anti-IRF-1 antibody (Santa Cruz Biotechnology, Santa Cruz, Calif.), followed by the addition of peroxidase-labeled anti-rabbit immunoglobulin G (IgG) antibody. Chemiluminescence was detected by using the ECL Western blotting analysis system (Amersham Biosciences, Buckinghamshire, United Kingdom) according to the manufacturer's protocol. The membrane was stripped by washing it with Tris-buffered saline containing 2% sodium dodecyl sulfate and 0.7% 2-mercaptoethanol for 30 min and then incubated with monoclonal anti-NS5A antibody (Biodesign, Saco, Maine), followed by the addition of peroxidase-labeled anti-mouse IgG antibody.

Preparation of a recombinant adenovirus expressing IRF-1. The PmeI-BamHI-digested fragment of pcDNA4/to/IRF-1-Myc/His containing the IRF-1 gene with a myc/His tag was blunt ended by using a DNA blunting kit (Takara, Otsu, Japan). This fragment was integrated to produce the IRF-1-expressing recombinant adenovirus vector, Ad-IRF-1 by using an adenovirus expression vector kit (Takara). The IRF-1 protein produced by Ad-IRF-1 had a myc/His tag that was used for differentiation from endogenous IRF-1. LacZ-expressing adenovirus, Ad-LacZ, was prepared as a control. The expression of IRF-1 from Ad-IRF-1 was confirmed by Western blot analysis. Cured Huh7 cells were infected with Ad-IRF-1 at multiplicity of infection (MOI) of 3. As a control, pcDNA3-IRF-1 and pcDNA4/to/IRF-1-Myc/His were transfected on cured Huh7 cells by using FuGENE-6. At 48 h after the transfection, nuclear extracts were prepared and Western blot analysis was performed by using anti-IRF-1 antibody and anti-His antibody as previously described.

Statistical analyses. Statistical analysis was performed by using an unpaired, two-tailed Student *t* test. *P* values of <0.05 were considered statistically significant.

RESULTS

ISRE activities in cells harboring the HCV replicon were lower than in naive Huh7. The ISRE and GAS activities of naive Huh7 cells and the Huh7 cell lines harboring the replicon (Huh7/Rep-N and Huh7/Rep-J4) were analyzed by transfection of the reporter constructs, pISRE-TA-Luc and pGAS-TA-Luc (Fig. 1A). The relative ISRE-regulated luciferase activities were significantly lower in the Huh7/Rep-N and Huh7/Rep-J4 cells than in untransfected Huh7 cells (22.6% ± 0.8% and 30.0% ± 1.9% in Huh/Rep-N and Huh7/Rep-J4 relative to naive Huh7 cells, respectively; $P < 0.0001$). On the other hand, the GAS-luciferase activities were at almost background levels in all cell lines tested. We also examined the ISRE responses to exogenous IFN-α stimuli in cells with or without replicon (Fig. 1B). At 6 h after treatment with 10 U of IFN-α/ml, induction levels of ISRE activity were not significantly different between cell lines (170.1% ± 31.2%, 203.8% ± 51.4%, and 224.3% ± 21.1% in the naive Huh7, Huh7/Rep-N and Huh7-RepJ4, respectively).

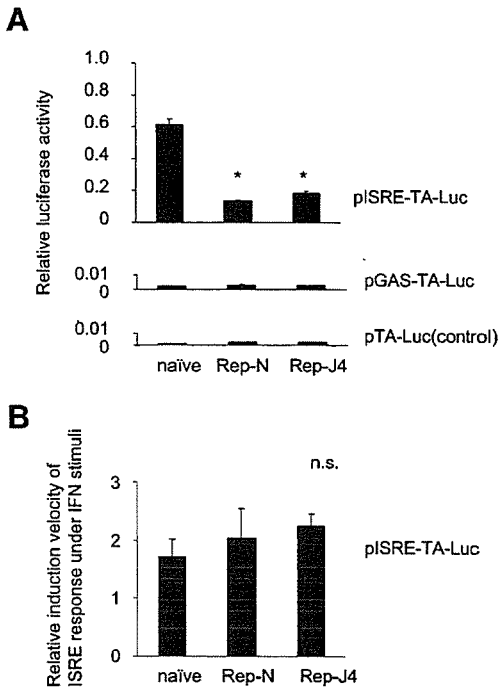

FIG. 1. ISRE activities in Huh7 cells and cells harboring the replicon. (A) The ISRE and GAS activities of naive Huh7 cells and Huh7 cells harboring the replicons (Huh7/Rep-N and Huh7/Rep-J4) were analyzed by reporter assays. These cells were transfected with pISRE-TA-Luc, pGAS-TA-Luc, and pTA-Luc, which lacks the enhancer element, as a control. pRL-CMV was cotransfected to correct the efficiency of transfection, and dual luciferase assays of the cell lysates were performed. The data are means ± the standard deviation (SD). ⋆, $P < 0.0001$ relative to naive Huh7 cells. (B) The ISRE responses to exogenous IFN-α stimuli in cells with or without replicon were analyzed by reporter assay. At 48 h after transfection with pISRE-TA-Luc and pRL-CMV, treatment with 10 U of IFN-α/ml was made. At 6 h after IFN-α stimuli, the relative induction levels of ISRE activities over each unstimulated cells were calculated.

IRF-1 expression was decreased in cells expressing the replicon. The ISRE activity is regulated by several known cellular factors (30, 38). To examine the levels of cellular factors that bind and regulate ISRE activity, we measured intracellular mRNA expression levels of IRF-1, IRF-3, STAT1-α, and STAT1-β in naive Huh7 and Huh7/Rep cells by RT-PCR analysis (Fig. 2A). The expression level of IRF-1 mRNA in Huh7

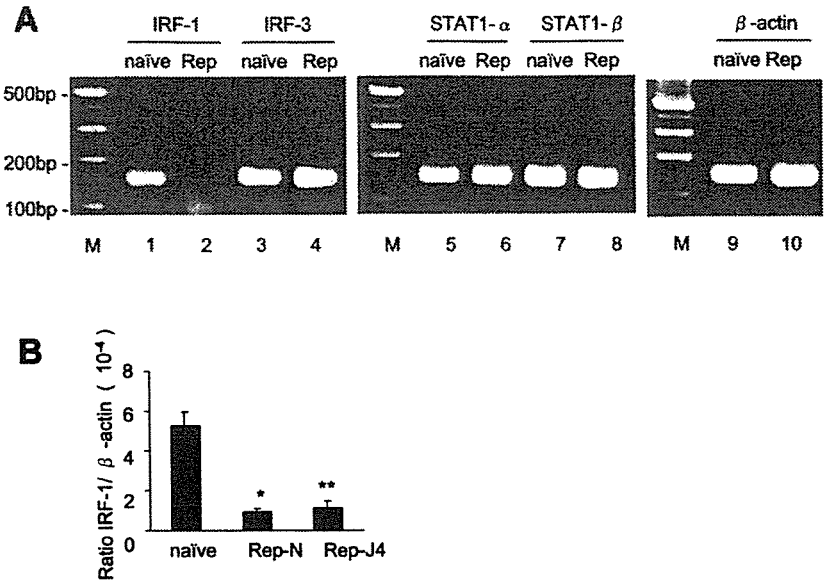

FIG. 2. The expression levels of IRF-1 mRNA were lower in cells harboring the replicon. (A) To determine the levels of cellular factors, we measured intracellular mRNA expression levels of IRF-1, IRF-3, STAT1-α, and STAT1-β in Huh7 and Huh7 cells harboring the replicon by RT-PCR analysis. (B) Quantification of the expression levels of interstitial IRF-1 mRNA was carried out by using real-time RT-PCR. cDNA was transcribed from naive Huh7 cells and cell lines harboring the replicon. Cycle numbers of the logarithmic linear phase were plotted against the logarithm of the concentration of template DNA and are presented as the calculated concentration in units. The data are means ± the SD. ⋆, P = 0.0013; ⋆⋆, P = 0.0022 (relative to naive Huh7 cells).

cells harboring the replicon was markedly decreased compared to that in naive Huh7. On the other hand, there were no differences in the expression levels of IRF-3, STAT1-α, and STAT1-β between cells with or without the replicon. The levels of IRF-1, IRF-3 and β-actin genes were quantified by using quantitative real-time RT-PCR and normalized by β-actin. The analysis showed that the expression levels of IRF-1 in the two Huh7 cell lines expressing the HCV replicon were significantly lower than in Huh7 cells (17.8% ± 3.2% and 21.9% ± 3.2% relative to naive Huh7 cells [P = 0.0013 and P = 0.0022 in Huh/Rep-N and Huh7/Rep-J4, respectively]; Fig. 2B). Also, in Western blot analysis, IRF-1 protein synthesis was decreased in Huh7 cells expressing replicon compared to naive Huh7 cells (see Fig. 5, lanes 1 to 3). These results suggest that the downregulation of the ISRE activities in cells expressing the replicon is mediated, at least in part, by a decrease in cellular IRF-1 transcription.

IRF-1 positively regulated the ISRE activity. It is known that IRF-1 binds directly not only to IRF-E but also to ISRE and positively regulates the expression of ISGs (27, 37). Therefore, we examined the effects of overexpression and suppression of IRF-1 on ISRE activity in cells expressing the HCV replicon. An IRF-1 expression vector, pcDNA3-IRF-1, was cotransfected with the pISRE-TA-Luc reporter construct into Huh7/Rep-N. After 48 h of transfection, the ISRE-driven luciferase activities were significantly higher, increasing in a dose-dependent manner up to ~90-fold in cells transfected with pcDNA3-IRF-1 (Fig. 3A).

Overexpression of IRF-1 suppressed expression of the HCV replicon. To examine the effect of IRF-1 expression on intracellular HCV replication, pcDNA3-IRF-1 was transfected into Huh7/Rep-Feo cells, in which the replicon expression levels can be monitored readily by luciferase assays. After transfection of pcDNA3-IRF-1 with empty vector, to a total mass of DNA of 400 ng, into Huh7/Rep-Feo cells, the luciferase activities of the Huh7/Rep-Feo decreased significantly in a dose-dependent manner (Fig. 4A). MTS assays of the cells transfected with IRF-1 showed no significant effects on cell growth and viability, demonstrating that the effects of IRF-1 transfection on the expression of the replicon were not due to cytotoxicity (Fig. 4B).

IRF-1 remains underexpressed in cured Huh7 cells. It has been reported that HCV proteins modulate the expression of various IFN-regulated genes (15, 20). To determine whether

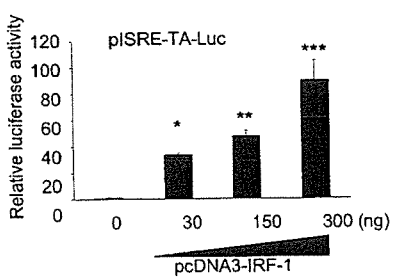

FIG. 3. Effect of IRF-1 overexpression and knockdown on the regulation of ISRE activity. The effects of IRF-1 on the regulation of ISRE activity were analyzed in cells expressing the HCV replicon. pRL-CMV (Promega) was cotransfected to correct for the efficiency of induction. Luciferase activities in Huh7/Rep-N cells cotransfected with pISRE-TA-Luc and various amounts of pcDNA3-IRF-1 with empty vector, to a total mass of DNA 400 ng, were assayed 48 h after transfection. The data are means ± the SD. ⋆, P = 0.004; ⋆⋆, P = 0.0023; ⋆⋆⋆, P = 0.0099 (relative to transfection with the empty vector).

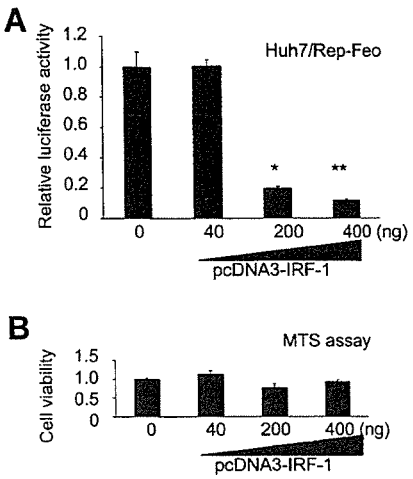

FIG. 4. Effect of IRF-1 overexpression on the replication of the HCV replicon. The effects of IRF-1 on the cells harboring the HCV replicon were analyzed. (A) Transfection of pcDNA3-IRF-1 into Huh7/Rep-Feo and monitoring of replication levels as luciferase activities in the cell lysates were performed. Empty vector was cotransfected to correct the amounts of transfected vectors to be same quantity, and single luciferase assays of the cell lysates were performed 48 h after transfection. The data are means ± the SD. ⋆, $P = 0.005$; ⋆⋆, $P = 0.0041$ (relative to transfection with the empty vector). (B) MTS assays of the cells transfected IRF-1.

the decrease of IRF-1 in the cells expressing replicon is due to negative regulatory effects of HCV nonstructural proteins, cured Huh7 cells were used from which the replicon had been removed. Equal amounts of nuclear extract from each were loaded in each lane to perform Western blot analysis of IRF-1 protein. Interestingly, IRF-1 expression in cured Huh7 cells remained decreased to levels similar to the Huh7 cells harboring the replicon (Fig. 5, lanes 2 through 4). Similarly, ISRE activities and expression levels of IRF-1 mRNA in cured Huh7 cells remained lower than in naive Huh7 cells and were similar to those in HCV cells harboring the replicon.

Overexpression of IRF-1 renders cured Huh7 cells nonpermissive for the HCV replicon. To determine whether the downregulation of IRF-1 enables replication of the HCV replicon, we performed transient-replication assays on the cured Huh7 cells. As reported earlier, the cured Huh7 cells showed increased permissiveness for replication of the HCV replicon (7) (Fig. 6A). The HCV replicon expressing firefly luciferase, Rep-Fluc, was transfected into the cured Huh7 cells and into naive Huh7 cells by electroporation. As a negative control, Rep-Fluc-NS5Bdel also was transfected into the cells. Transfection of the replication-deficient construct, Rep-Fluc-NS5Bdel, showed that the luciferase activity, which was maximal at 4 h, diminished subsequently and reached background levels by 72 h. In contrast, transfection of Rep-Fluc into the cured and naive Huh7 showed that the luciferase activity, once decreased, became elevated again at 48 and 72 h, demonstrating obvious replication. The luciferase activities of the cured Huh7 cells at 48 and 72 h were significantly higher than those of naive Huh7 cells. These results showed that the cured Huh7 cells were highly permissive compared to naive Huh7 cells.

To examine the effect of IRF-1 supplementation on the cured Huh7 cells, IRF-1-expressing recombinant adenovirus, Ad-IRF-1, was constructed from pcDNA4/to/IRF-1-Myc/His that expresses IRF-1 with the myc-His tag. The expression of IRF-1 in the cured Huh7 cells was examined by Western blot analysis (Fig. 6B). In lysates derived from Ad-IRF-1-infected cells (Fig. 6B, lane 1) and pcDNA4/to/IRF-1-Myc/His-transfected cells (Fig. 6B, lane 2), IRF-1 was detected by both anti-IRF-1 antibody and anti-His antibody. The molecular weights of these IRF-1s are higher thanthat of the IRF-1 derived from pcDNA3-IRF-1 by the addition of myc-His tag (Fig. 6B, lane 3). Various titers of Ad-IRF-1 were used to infect the cured Huh7 cells 3 h before electroporation of Rep-Fluc (Fig. 6C). The relative values of 72 h divided by those for 4 h were calculated. Adenovirus transfection of IRF-1 suppressed the replication of the HCV replicon in the cured Huh7 cells in a dose-dependent manner (Fig. 6C, lanes 2 to 5). Infection of the cured Huh7 cells with Ad-IRF-1 at an MOI of 3 resulted in a loss of permissiveness for the replicon by about 20% (2.0 ± 0.1 and 0.4 ± 0.1, respectively) (Fig. 6C, lanes 1 and 5). To determine whether overexpression of IRF-1 affected the permissiveness of the cured Huh7 cells, a transient assay was performed by using an siRNA directed to IRF-1 mRNA. The cured Huh7 cells were infected with Ad-IRF-1 at an MOI of 10. Rep-Fluc and the siRNA were cotransfected 3 h after infection, and the luciferase activities were measured at 4 and 72 h after transfection. The replication of the HCV replicon was increased by knockdown of IRF-1 in a dose-dependent manner (Fig. 6D).

DISCUSSION

This is the first study of the involvement of IRF-1 in HCV replication. Using Huh7 cell lines harboring an HCV replicon and cells cured of the replicon, we have found that the baseline ISRE activity of cells harboring the HCV replicon is lower than that of naive cells (Fig. 1A). Among the host proteins that bind and regulate ISRE activity, expression of IRF-1 alone was decreased in the cells harboring the replicon (Fig. 2). Because overexpression analyses of IRF-1 have been shown to affect ISRE activity directly (Fig. 3), the transcriptional decrease of IRF-1 in the cells expressing the replicon appears to attenuate

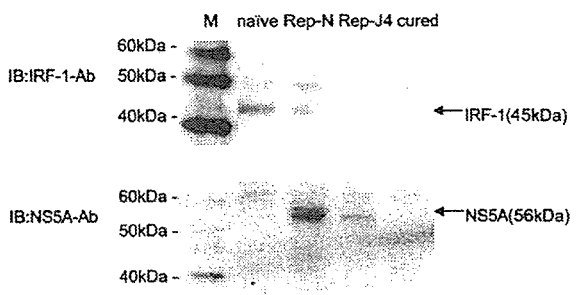

FIG. 5. Western blot analysis of IRF-1 and NS5A expression in naive Huh7 cells, Huh7/Rep-N and Huh7/Rep-J4 cells, and cured Huh7 cells. Nuclear extracts were isolated from naive Huh7 cells, Huh7 cells harboring the replicons, and cured Huh7 cells. A total of 25 μg of each was separated on a sodium dodecyl sulfate–10% polyacrylamide gel and immunoblotted with anti-IRF-1 antibody. The membrane was reprobed with a rabbit anti-NS5A antibody and analyzed. IB, immunoblotting with the indicated primary antibody.

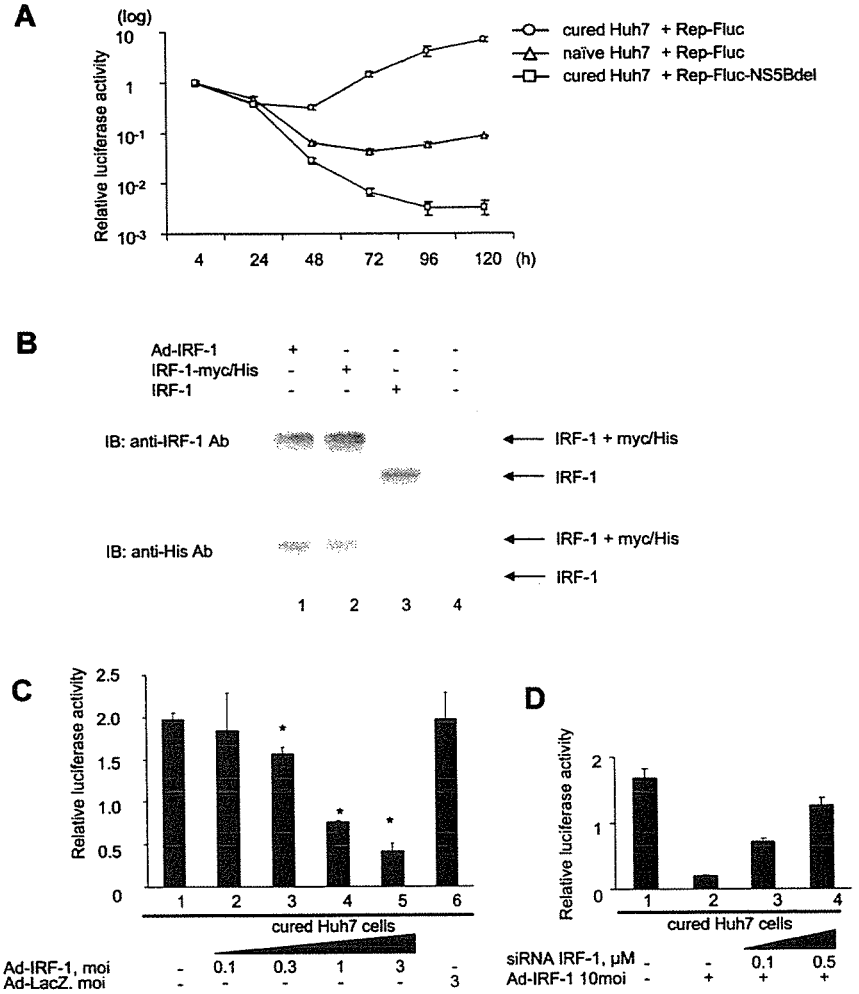

FIG. 6. Cured Huh7 cells lost their permissiveness for the HCV replicon with overexpression of IRF-1. Transient replication assays were performed on cured Huh7 cells to determine whether the downregulation of IRF-1 enables replication of the HCV replicon. (A) The high permissiveness of cured Huh7 cells is shown. The HCV replicon expressing the firefly luciferase, Rep-Fluc, was transfected into cured Huh7 cells and naive Huh7 cells by electroporation. As a negative control, Rep-Fluc-NS5Bdel also was transfected into the cells. The luciferase activities of the cell lysates were measured. To correct for the efficiency of induction, each value is shown as a ratio relative to the relevant relative light units at 4 h. (B) The IRF-1 protein produced by IRF-1-expressing recombinant adenovirus, Ad-IRF-1, was examined. Cured Huh7 cells were infected at an MOI of 3 with Ad-IRF-1 (lane 1). As a control, pcDNA3-IRF-1 (lane 2) and pcDNA4/to/IRF-1-Myc/His (lane 3) were transfected on cured Huh7 cells by using FuGENE-6. At 48 h after transfection, nuclear extracts were isolated and Western blot analysis was performed with anti-IRF-1 antibody and anti-His antibody, as previously described. (C) To determine the effect of supplementation of IRF-1 on the cured Huh7 cells, various titers of Ad-IRF-1 were used to infect the cured Huh7 cells 3 h before electroporation of Rep-Fluc. The relative values of 72 h over 4 h were calculated. The data are means ± the SD. ⋆, $P < 0.01$ (relative to null transfection [lane 1]). (D) To determine whether overexpression of IRF-1 affected the permissiveness of the cured Huh7 cells, a transient assay was performed with an siRNA directed to IRF-1 mRNA. At 3 h before electroporation, the cured Huh7 cells were infected with Ad-IRF-1 at MOI of 10. Rep-Fluc and the siRNA oligonucleotide directed to IRF-1 were transfected by electroporation. The relative values of 72 h over 4 h were calculated.

ISG responses mediated by the ISRE. Indeed, the overexpression of IRF-1 suppressed replication of the HCV replicon substantially (Fig. 4). One possible explanation was that the decrease in IRF-1 expression was due to active suppression by viral proteins. We found that, although IRF-1 seemed to have been suppressed by the HCV replicon, the cured Huh7 cells, from which the replicon had been eliminated, also showed decreased ISRE activity and a lower expression level of IRF-1 mRNA (Fig. 5). These results suggest that the decrease in IRF-1 found in our present study is not due to active downregulation by expression of viral proteins but possibly to the adaptation of the host cells to increased permissiveness for the replicon through continuous selection of the replicon during culture with G418. Transgenic supplementation of IRF-1 into cured Huh7 cells again abolished their high permissiveness for the replicon (Fig. 6C). Taking all of these findings into consideration, IRF-1 is one of the key cellular factors that modulate levels of ISRE-regulated ISG expression and predominantly affect the intracellular replication of HCV genomic RNA.

Induction of ISGs is mediated through ISRE and/or GAS (11, 39). Our initial results from a reporter assay showed that the ISRE activity in the absence of IFN stimuli was significantly lower in cells harboring the replicon than in naive cells. On the other hand, the activities of GAS were at almost background levels in both naive cells and cells harboring the replicon, suggesting that IFN-γ and the GAF/GAS pathway are much less involved in the cellular antiviral actions in Huh7 cells (Fig. 1). ISRE is bound by ISGF-3 or by IRFs. However, in the absence of IFN stimuli, ISGF-3 is not the main activating factor for ISRE (24). Thus, the IRFs, including IRF-1, IRF-3, and IRF-7, are potential regulators of the baseline ISRE activity. Our present results have shown that IRF-1 was suppressed exclusively in cells harboring the replicon (Fig. 2). These results suggest that the decreased ISRE activity found in the cells harboring the replicon may be attributable to the transcriptional decrease of IRF-1.

The HCV structural and nonstructural proteins have been reported to affect the IFN signaling pathway. Heim et al. reported that expression of the entire HCV polyprotein in Huh7 cells strongly inhibited IFN-α-mediated signal transduction (18). Stable expression of HCV core protein inhibited IFN-induced STAT1 expression through modulation of both GAF and ISGF-3 protein complex formation, but it did not interfere with the activation of the downstream effector genes, IRF-1 and 561, in IFN-treated cells (4). IFN-induced intracellular signaling through the Jak/STAT pathway is impaired in a transgenic mouse that expresses the HCV protein (8). Pflugheber et al. have reported that intracellular expression of NS5A blocks activation of IRF-1 triggered by double-stranded RNA and that those effects play a part in viral persistence (26b). These reports suggested that interference with IFN-induced intracellular signaling by HCV proteins could be the explanation for HCV resistance to IFN treatment.

The expression levels of mRNA are not only controlled by transcriptional regulation but also through posttranscriptional effects such as modulation of mRNA stability. As for IRF-1, several studies have shown that the expression is regulated by transcriptional modulation principally through STATs and NF-κB (17, 29). Our preliminary data of mRNA stability assay by actinomycin D treatment, an inhibitor of transcription elongation, failed to detect a difference in the half-life of IRF-1 mRNA between cell lines with or without the replicon.

We do not have a satisfactory explanation of why IRF-1 was the primary target of clonal knockdown in the cells harboring the replicon. Because IRF-1 has important roles in the antiviral mechanism (14, 21, 30), the lower expression of IRF-1 might be enough to achieve high levels of continuous cellular replication of the HCV replicon. Blight et al. reported that cured Huh7 cells are highly permissive for HCV replication and suggested that the difference in permissiveness of the cured Huh7 cells for HCV replication might be explained by a subpopulation of the parental Huh7 cells that are permissive for replication of the HCV replicon (7). Interestingly, they also have reported that the permissiveness of parental naive Huh7 cells was not altered by treatment with IFN. These results suggest that one of the factors governing permissiveness for the HCV replicon may be induced by the selection of cells with lower levels of IRF-1 expression. Indeed, the overexpression of IRF-1 in the cured Huh7 cells removed the permissiveness for the HCV replicon in parallel with the expression of the transfected IRF-1. It is also possible that a subpopulation of Huh-7 cells, which express lower levels of IRF-1, may subsequently be selected through the antibiotic selection. However, our data have shown that a typical transfection of 5 μg of replicon RNA into 6×10^6 of Huh7 cells yields more than 1,000 G418-resistant colonies and that the numbers of the colonies correlate with the amount of the transfected replicon RNA and not with the numbers of cells seeded. These findings suggest that the decrease in IRF-1 expression in replicon-harboring Huh7 is not due to the selection of cells in which IRF-1 is genetically knocked down.

It has recently been reported that other nonhepatic human cell lines and mouse hepatic cells could also harbor a subgenomic replicon (2, 12, 19, 42). We have performed a preliminary study with an HCV replicon derived from HCV genotype 2a, JFH-1, which replicates in various hepatic and nonhepatic cell lines (12, 19). An assay with human epithelial HeLa cells expressing JFH-1 replicon has shown that the relative ISRE activity was significantly lower in the HeLa/JFH-1 cells than in untransfected HeLa cells (52.4% ± 3.5% in HeLa/JFH-1 cells relative to naive HeLa cells). However, the baseline expression level of IRF-1 mRNA was much lower in HeLa cells with or without replicon than that in Huh7 cells. Although further studies are necessary, our findings suggest that the decreased baseline ISRE activities may at least have contributed to permissiveness and high-level expression of HCV replicon and that the decreased IRF-1 activities may be one mechanism to downregulate ISRE activities in Huh7 cells.

In contrast to the results in cultured cells, the clinical features of IFN, ISGs, and IRF expression are complicated. A study with needle biopsy samples from chronic hepatitis C patients who had not been treated with IFN showed that IFN-γ and IRF-1 mRNA were upregulated and correlated positively with the patients' alanine aminotransferase levels in blood (1). Another group reported that peripheral blood mononuclear cells from patients with hepatitis C showed increased expression of IRF-1 mRNA and higher IRF-1/IRF-2 ratios compared to normal subjects (23). A possible reason for the discrepancy in IRF-1 expression patterns between clinical samples and the replicon cell culture system may be the presence or absence of the immune system. IFN-γ, which is known to be the strongest inducer of IRF-1 (22), is synthesized by natural killer cells, CD4 Th1 cells, and CD8 cytotoxic lymphocytes in response to antigenic stimuli (34). In any case, it has been suggested that IRF-1 is one of the principal host factors involved in cellular responses against viral infection and in clearance of viruses from cells.

In conclusion, our results demonstrate that IRF-1 is an important regulatory factor for baseline HCV replication and has a widely accepted role as a mediator of antiviral action. IRF-1 potentially may be a key molecular target to control HCV replication.

REFERENCES

1. **Abbate, I., M. Romano, R. Longo, G. Cappiello, O. Lo Iacono, V. Di Marco, C. Paparella, A. Spano, and M. R. Capobianchi.** 2003. Endogenous levels of mRNA for IFNs and IFN-related genes in hepatic biopsies of chronic HCV-infected and non-alcoholic steatohepatitis patients. J. Med. Virol. 70:581–587.
2. **Ali, S., C. Pellerin, D. Lamarre, and G. Kukolj.** 2004. Hepatitis C virus

subgenomic replicons in the human embryonic kidney 293 cell line. J. Virol. **78**:491–501.
3. **Alter, M. J.** 1997. Epidemiology of hepatitis C. Hepatology **26**:62S–65S.
4. **Basu, A., K. Meyer, R. B. Ray, and R. Ray.** 2001. Hepatitis C virus core protein modulates the interferon-induced transacting factors of Jak/Stat signaling pathway but does not affect the activation of downstream IRF-1 or 561 gene. Virology **288**:379–390.
5. **Bigger, C. B., K. M. Brasky, and R. E. Lanford.** 2001. DNA microarray analysis of chimpanzee liver during acute resolving hepatitis C virus infection. J. Virol. **75**:7059–7066.
6. **Blight, K. J., A. A. Kolykhalov, and C. M. Rice.** 2000. Efficient initiation of HCV RNA replication in cell culture. Science **290**:1972–1974.
7. **Blight, K. J., J. A. McKeating, and C. M. Rice.** 2002. Highly permissive cell lines for subgenomic and genomic hepatitis C virus RNA replication. J. Virol. **76**:13001–13014.
8. **Blindenbacher, A., F. H. Duong, L. Hunziker, S. T. Stutvoet, X. Wang, L. Terracciano, D. Moradpour, H. E. Blum, T. Alonzi, M. Tripodi, N. La Monica, and M. H. Heim.** 2003. Expression of hepatitis C virus proteins inhibits interferon alpha signaling in the liver of transgenic mice. Gastroenterology **124**:1465–1475.
9. **Bukh, J., T. Pietschmann, V. Lohmann, N. Krieger, K. Faulk, R. E. Engle, S. Govindarajan, M. Shapiro, M. St Claire, and R. Bartenschlager.** 2002. Mutations that permit efficient replication of hepatitis C virus RNA in Huh-7 cells prevent productive replication in chimpanzees. Proc. Natl. Acad. Sci. USA **99**:14416–14421.
10. **Choo, Q. L., G. Kuo, A. J. Weiner, L. R. Overby, D. W. Bradley, and M. Houghton.** 1989. Isolation of a cDNA clone derived from a blood-borne non-A, non-B viral hepatitis genome. Science **244**:359–362.
11. **Darnell, J.E., Jr., I. M. Kerr, and G. R. Stark.** 1994. Jak-STAT pathways and transcriptional activation in response to IFNs and other extracellular signaling proteins. Science **264**:1415–1421.
12. **Date T., T. Kato, M. Miyamoto, Z. Zhao, K. Yasui, M. Mizokami, and T. Wakita.** 2004. Genotype 2a hepatitis C virus subgenomic replicon can replicate in HepG2 and IMY-N9 cells. J. Biol. Chem. **279**:22371–22376.
13. **Frese, M., T. Pietschmann, D. Moradpour, O. Haller, and R. Bartenschlager.** 2001. Interferon-alpha inhibits hepatitis C virus subgenomic RNA replication by an MxA-independent pathway. J. Gen. Virol. **82**:723–733.
14. **Frese, M., K. Barth, A. Kaul, V. Lohmann, V. Schwarzle, and R. Bartenschlager.** 2003. Hepatitis C virus RNA replication is resistant to tumour necrosis factor-alpha. J. Gen. Virol. **84**:1253–1259.
15. **Geiss, G. K., V. S. Carter, Y. He, B. K. Kwieciszewski, T. Holzman, M. J. Korth, C. A. Lazaro, N. Fausto, R. E. Bumgarner, and M. G. Katze.** 2003. Gene expression profiling of the cellular transcriptional network regulated by alpha/beta interferon and its partial attenuation by the hepatitis c virus nonstructural 5A protein. J. Virol. **77**:6367–6375.
16. **Guo, J. T., V. V. Bichko, and C. Seeger.** 2001. Effect of alpha interferon on the hepatitis C virus replicon. J. Virol. **75**:8516–8523.
17. **Harada, H., E. Takahashi, S. Itoh, K. Harada, T. A. Hori, and T. Taniguchi.** 1994. Structure and regulation of the human interferon regulatory factor 1 (IRF-1) and IRF-2 genes: implications for a gene network in the interferon system. Mol. Cell. Biol. **14**:1500–1509.
18. **Heim, M. H., D. Moradpour, and H. E. Blum.** 1999. Expression of hepatitis C virus proteins inhibits signal transduction through the Jak-STAT pathway. J. Virol. **73**:8469–8475.
19. **Kato, T., T. Date, M. Miyamoto, A. Furusaka, K. Tokushige, M. Mizokami, and T. Wakita.** 2003. Efficient replication of the genotype 2a hepatitis C virus subgenomic replicon. Gastroenterology **125**:1808–1817.
20. **Katze, M. G., Y. He, and M. Gale, Jr.** 2002. Viruses and interferon: a fight for supremacy. Nat. Rev. Immunol. **2**:675–687.
21. **Kimura, T., K. Nakayama, J. Penninger, M. Kitagawa, H. Harada, T. Matsuyama, N. Tanaka, R. Kamijo, J. Vilcek, and T. W. Mak.** 1994. Involvement of the IRF-1 transcription factor in antiviral responses to interferons. Science **264**:1921–1924.
22. **Kroger, A., M. Koster, K. Schroeder, H. Hauser, and P. P. Mueller.** 2002. Activities of IRF-1. J. Interferon Cytokine Res. **22**:5–14.
23. **Larrea, E., A. Alberdi, Y. Castelruiz, P. Boya, M. P. Civeira, and J. Prieto.** 2001. Expression of interferon-alpha subtypes in peripheral mononuclear cells from patients with chronic hepatitis C: a role for interferon-α5. J. Viral. Hepat. **8**:103–110.
24. **Lau, J. F., J. P. Parisien, and C. M. Horvath.** 2000. Interferon regulatory factor subcellular localization is determined by a bipartite nuclear localization signal in the DNA-binding domain and interaction with cytoplasmic retention factors. Proc. Natl. Acad. Sci. USA **97**:7278–7283.
25. **Lohmann, V., F. Korner, J. Koch, U. Herian, L. Theilmann, and R. Bartenschlager.** 1999. Replication of subgenomic hepatitis C virus RNAs in a hepatoma cell line. Science **285**:110–113.
25a. **Maekawa, S., N. Enomoto, N. Sakamoto, M. Kurosaki, E. Ueda, T. Kohashi, H. Watanabe, C. H. Chen, T. Yamashiro, Y. Tanabe, N. Kanazawa, M. Nakagawa, C. Sato, and M. Watanabe.** Introduction of NS5A mutations enables subgenomic HCV-replicon derived from chimpanzee-infectious HC-J4 isolate to replicate efficiently in Huh-7 cells. J. Viral Hepatitis. in press.
26. **Nakaya, T., M. Sato, N. Hata, M. Asagiri, H. Suemori, S. Noguchi, N. Tanaka, and T. Taniguchi.** 2001. Gene induction pathways mediated by distinct IRFs during viral infection. Biochem. Biophys. Res. Commun. **283**: 1150–1156.
26a. **Oshima S., T. Nakamura, S. Namiki, E. Okada, K. Tsuchiya, R. Okamoto, M. Yamazaki, T. Yokota, M. Aida, Y. Yamaguchi, T. Kanai, H. Handa, and M. Watanabe.** Interferon regulatory factor 1 (IRF-1) and IRF-2 distinctively up-regulate gene expression and production of interleukin-7 in human intestinal epithelial cells. Mol. Cell. Biol., in press.
26b. **Pflugheber, J., B. Fredericksen, R. Sumpter, Jr., C. Wang, F. Ware, D. L. Sodora, and M. Gale, Jr.** 2002. Regulation of PKR and IRF-1 during hepatitis C virus RNA replication Proc. Natl. Acad. Sci. USA **99**:4650–4655.
27. **Pine, R., T. Decker, D. S. Kessler, D. E. Levy, and J. E. Jr Darnell.** 1990. Purification and cloning of interferon-stimulated gene factor 2 (ISGF2): ISGF2 (IRF-1) can bind to the promoters of both beta interferon- and interferon-stimulated genes but is not a primary transcriptional activator of either. Mol. Cell. Biol. **10**:2448–2457.
28. **Pine, R.** 1992. Constitutive expression of an ISGF2/IRF1 transgene leads to interferon-independent activation of interferon-inducible genes and resistance to virus infection. J. Virol. **66**:4470–4478.
29. **Pine, R., A. Canova, and C. Schindler.** 1994. Tyrosine phosphorylated p91 binds to a single element in the ISGF2/IRF-1 promoter to mediate induction by IFN alpha and IFN gamma and is likely to autoregulate the p91 gene. EMBO. J. **13**:158–167.
30. **Samuel, C. E.** 2001. Antiviral actions of interferons. Clin. Microbiol. Rev. **14**:778–809.
31. **Sato, M., N. Hata, M. Asagiri, T. Nakaya, T. Taniguchi, and N. Tanaka.** 1998. Positive feedback regulation of type I IFN genes by the IFN-inducible transcription factor IRF-7. FEBS Lett. **441**:106–110.
32. **Sato, M., H. Suemori, N. Hata, M. Asagiri, K. Ogasawara, K. Nakao, T. Nakaya, M. Katsuki, S. Noguchi, N. Tanaka, and T. Taniguchi.** 2000. Distinct and essential roles of transcription factors IRF-3 and IRF-7 in response to viruses for IFN-alpha/beta gene induction. Immunity **13**:539–548.
33. **Sen, G. C.** 2001. Viruses and interferons. Annu. Rev. Microbiol. **55**:255–281.
34. **Shtrichman, R., and C. E. Samuel.** 2001. The role of gamma interferon in antimicrobial immunity. Curr. Opin. Microbiol. **4**:251–259.
35. **Stark, G. R., I. M. Kerr, B. R. Williams, R. H. Silverman, and R. D. Schreiber.** 1998. How cells respond to interferons. Annu. Rev. Biochem. **67**:227–264.
36. **Tanabe, Y., N. Sakamoto, N. Enomoto, M. Kurosaki, E. Ueda, S. Maekawa, T. Yamashiro, M. Nakagawa, C. H. Chen, N. Kanazawa, S. Kakinuma, and M. Watanabe.** 2004. Synergistic inhibition of intracellular hepatitis C virus replication by combination of ribavirin and interferon-alpha. J. Infect. Dis. **189**:1129–1139.
37. **Tanaka, N., T. Kawakami, and T. Taniguchi.** 1993. Recognition DNA sequences of interferon regulatory factor 1 (IRF-1) and IRF-2, regulators of cell growth and the interferon system. Mol. Cell. Biol. **13**:4531–4538.
38. **Taniguchi, T., K. Ogasawara, A. Takaoka, and N. Tanaka.** 2001. IRF family of transcription factors as regulators of host defense. Annu. Rev. Immunol. **19**:623–655.
39. **Taniguchi, T., and A. Takaoka.** 2002. The interferon-alpha/beta system in antiviral responses: a multimodal machinery of gene regulation by the IRF family of transcription factors. Curr. Opin. Immunol. **14**:111–116.
40. **Yanagi, M., M. St Claire, M. Shapiro, S. U. Emerson, R. H. Purcell, and J. Bukh.** 1998. Transcripts of a chimeric cDNA clone of hepatitis C virus genotype 1b are infectious in vivo. Virology **244**:161–172.
41. **Yokota, T., N. Sakamoto, N. Enomoto, Y. Tanabe, M. Miyagishi, S. Maekawa, L. Yi, M. Kurosaki, K. Taira, M. Watanabe, and H. Mizusawa.** 2003. Inhibition of intracellular hepatitis C virus replication by synthetic and vector-derived small interfering RNAs. EMBO. Rep. **4**:602–608.
42. **Zhu, Q., J. T. Guo, and C. Seeger.** 2003. Replication of hepatitis C virus subgenomes in nonhepatic epithelial and mouse hepatoma cells. J. Virol. **77**:9204–9210.

Journal of Viral Hepatitis, 2004, **11**, 394–403

Introduction of NS5A mutations enables subgenomic HCV replicon derived from chimpanzee-infectious HC-J4 isolate to replicate efficiently in Huh-7 cells

S. Maekawa,[1] N. Enomoto,[1] N. Sakamoto,[1] M. Kurosaki,[1] E. Ueda,[1] T. Kohashi,[1] H. Watanabe,[1] C.-H. Chen[1],T. Yamashiro[1],Y. Tanabe[1],N. Kanazawa[1],M. Nakagawa[1], C. Sato[2] and M. Watanabe[1] *Departments of [1]Gastroenterology and Hepatology, and [2]Analytical Health Science, Tokyo Medical and Dental University, Tokyo, Japan*

Received September 2003; accepted for publication December 2003

SUMMARY. Hepatitis C virus (HCV) subgenomic replicon has been reported to replicate efficiently and continuously in human hepatoma Huh-7 cells. To extend the previous results to other isolated HCV clones, we constructed another HCV replicon from HC-J4, one of chimpanzee-infectious HCV clones. An HCV replicon derived from HC-J4 (RpJ4) consists of HCV-5′ untranslated region, neomycin phosphotransferase gene, the encephalomyocarditis virus internal ribosomal entry site, HCV nonstructural region, NS3 to NS5B, and HCV-3′ untranslated region. The adaptive mutations known to be required for HCV-Con1 replicon were introduced in RpJ4 replicon, aa.(amino acids number according to HC-J4) 2197 serine to proline, deletion of serine at aa.2201, and aa.2204 serine to isoleucine (RpJ4-S2197P, RpJ4-S22001del, and RpJ4-S2204I). RpJ4/ISDR mutant and RpJ4-S2201del/ISDR mutant were also constructed by introducing six amino acid mutations into the interferon sensitivity determining region (ISDR). After transfection into Huh-7 cells and G418 selection, RpJ4 and RpJ4/ISDR mutants did not produce any colony. In contrast, G418-resistant cells were transduced efficiently by RpJ4-S2197P, RpJ4-S2204I, RpJ4-S2201del and RpJ4-S2201del/ISDR mutant, with the RpJ4-S2201del/ISDR mutant being most efficient. Hence the HCV replicon derived from HC-J4 can replicate efficiently following the introduction of adaptive mutations into the upstream region of ISDR. Moreover, additional introduction of mutations into ISDR further enhanced its replication. These findings demonstrate that the genetic structure of the NS5A domain is critical in HCV replications.

Keywords: adaptive mutations, cell culture system, interferon sensitivity determining region, serine cluster region.

INTRODUCTION

Hepatitis C Virus (HCV) is the major causative agent of chronic liver diseases leading to cirrhosis two to three decades after infection. Furthermore, 1–4% of such cases subsequently develop hepatocellular carcinoma annually [1]. Anti-viral therapies for HCV eradicate the virus in only half of the treated individuals, including the combination therapy of interferon plus ribavirin, currently the most powerful regimen [2,3]. Cell culture systems that simulate HCV replication are essential to elucidate the mechanism of viral replication and to develop antiviral strategies. Recently, a subgenomic HCV replicon system was established by replacing HCV structural protein genes with the neomycin phosphotransferase (Neo) gene, followed by an internal ribosomal entry site (IRES) of the encephalomyocarditis virus (EMCV). This HCV replicon replicates autonomously in human hepatoma Huh-7 cells through G418-selection [4].

Despite the success of the HCV replicon, several features of this replicon system remain unexplained. First, functional replicons are limited to several HCV-1b clones (Con1, HCV-N, M1LE and HCV-BK) [4–8], one HCV-1a clone (H77) [9], or one HCV-1a/1b chimera clone (H77/Con1 chimera) [10]. This limitation raises a question of whether the replicon system merely reflects characteristics specific to these limited HCV isolates. In addition, designated cell culture-adaptive amino acid mutations in nonstructural (NS) regions are required for their efficient replication [11–14]. Despite the

Abbreviations: AGPC, acid guanidium/phenol/chloroform; CFU, colony-forming unit; DMEM, Dulbecco's modified minimal essential medium; EMCV, encephalomyocarditis virus; HCV, hepatitis C virus; Huh-7, human hepatoma cells; IRES, internal ribosomal entry site; ISDR, interferon sensitivity determining region; NS, nonstructural; RT-PCR, reverse transcriptase-polymerase chain reaction; UTR, untranslated region.

Correspondence: Nobuyuki Enomoto, Department of Gastroenterology and Hepatology, Tokyo Medical and Dental University, 1-5-45 Yushima, Bunkyo, Tokyo 113-8519, Japan. E-mail: nenomoto.gast@tmd.ac.jp